SACLANTCEN Memorandum
SM - 155

SACLANT ASW RESEARCH CENTRE MEMORANDUM

ON THE USE OF DOUBLE FM PULSES FOR DETECTION OF TARGETS AND MEASUREMENT OF THEIR PROPERTIES

by

LEWIS MEIER

15 NOVEMBER 1981

NORTH ATLANTIC TREATY ORGANIZATION

LA SPEZIA, ITALY

Published by

STI

SACLANTCEN MEMORANDUM SM-155

NORTH ATLANTIC TREATY ORGANIZATION

SACLANT ASW Research Centre
Viale San Bartolomeo 400, I-19026 San Bartolomeo (SP), Italy.

national 0187 560940
international + 39 187 560940

telex: 271148 SACENT I

ON THE USE OF DOUBLE FM PULSES FOR DETECTION OF TARGETS AND MEASUREMENT OF THEIR PROPERTIES

by

Lewis Meier

15 November 1981

This memorandum has been prepared within the SACLANTCEN
Systems Research Division as part of Project 02.

L.F. WHICKER
Division Chief

TABLE OF CONTENTS

		Pages
ABSTRACT		1
INTRODUCTION		1
1	BACKGROUND	3
2	RESOLUTION	12
3	SINGLE-ECHO DETECTION	14
	3.1 Point Targets	14
	3.2 Distributed Targets	15
4	INCOHERENT MEASUREMENTS	17
	4.1 Basic Measurement Principle	17
	4.2 Plaisant's Approach to Estimation of Modulation Delays and Spreads	19
	4.3 Standard Deviations and Means of the Measurement Errors	23
	4.4 Selection of Signal and Signal-Processing Parameters	24
5	COHERENT MEASUREMENTS	27
	5.1 Basic Measurement Principle	27
	5.2 Plaisant's Approach to Estimation of the Correlation Peak	31
	5.3 Measurement Error Means and Standard Deviation	33
	5.4 Selection of Signal and Signal-Processing Parameters	33
	5.5 Comparison of Coherent and Incoherent Measurements	35
6	SPACE/FREQUENCY MEASUREMENTS	35
	6.1 Basic Measurement Principle	36
	6.2 Plaisant's Approach to Estimation of the Correlation Peak	40
	6.3 Means and Standard Deviation of the Measurement Error	41
	6.4 Selection of Signal and Signal-Processing Parameters	42
7	ALGORITHMS	43
	7.1 Estimation of Background Power	44
	7.2 Single-Echo Detection	44
	7.3 Incoherent Measurement Extraction	44
	7.4 Coherent Algorithms	45
	7.5 Space/Frequency Algorithms	46
	7.6 Multiple-Echo Detection	46
CONCLUSIONS		47
REFERENCES		49

TABLE OF CONTENTS (Cont'd)

	Pages
APPENDIX A - SPREAD OF DOPPLER AMBIGUITY FUNCTION IN TIME	51
APPENDIX B - DETERMINATION OF THE DOPPLER SHIFT CAUSING THE PEAK MATCHED-FILTER OUTPUT POWER TO FALL BY HALF	53
APPENDIX C - STANDARD DEVIATION OF THE HALF-ECHO-POWER POINTS	55
APPENDIX D - STANDARD DEVIATION OF THE 50% CORRELATION POINTS	61

List of Figures

1.	Matched filter output for FM pulse and line target	3
2.	Matched filter output for double FM pulse and line target	8
3.	Resolution for $y = 0.84$	13
4.	y^* vs $\|x\|$	16
5.	Path length error standard deviation for example	26
6a.	Apparent turning rate error standard deviation for example	37
6b.	Path length rate error standard deviation for example	37
7.	Estimating echo-plus-noise power level and finding the half-echo-power times	37

ON THE USE OF DOUBLE FM PULSES FOR DETECTION OF TARGETS AND MEASUREMENT OF THEIR PROPERTIES

by

Lewis Meier

ABSTRACT

This report discusses the use of double FM pulses to measure the sonar path length and rate of change of sonar path length (range and range rate in the monostatic case) and length and rate of change of length or apparent turning rate for a long thin target such as a submarine. Equations are derived for the standard deviations of the errors of such measurements. It is shown that for coherent processing roof top double FM pulses are preferred while for incoherent processing parallel, double FM pulses are preferred. This report further discusses the use of two hydrophones with the double FM pulse to measure, in addition to the above, bearing and aspect of the target. In this case coherent spatial processing is used that is exactly analogous to the coherent temporal processing. Again equations for the standard deviations of the errors in these measurements are derived.

INTRODUCTION

The major problem in submarine detection is to obtain a large enough signal-to-background ratio to reliably distinguish targets from noise. One solution is bigger and better transducers, but there is a limit to the amount of sound that may be forced into the water and, anyway, at a certain point one becomes reverberation limited and beyond this point increased power is of no avail. One way out of this difficulty is the use of multiple pulses [1]: if the echoes from the pulse are added incoherently, the signal-to-background ratio is unchanged but the variances of the background and the signal-plus-background are reduced – thus improving detection performance. If the echoes from the pulse are added coherently not only are the variances reduced, but

the signal-to-background ratio is increased — thus yielding an even greater improvement in detection performance. Note, however, that this procedure works better in the noise-limited use, since in the reverberation-limited case each pulse is in the reverberation of the other pulses. The same effect as the use of a multiple pulse can be obtained by the use of multiple hydrophones spaced sufficiently far apart that the noise on each is independent. In this case, naturally, there are no special problems caused by the reverberation limitations.

Adding echoes coherently is not always a straightforward task. For example, adding the ouputs of a linear array of hydrophones will not work unless the target is broadside to the array — in general, the hydrophone outputs must be appropriately shifted in time to add the echoes coherently. Such difficulties are also an opportunity, because they are usually intimately related to some property of the target — such as bearing with respect to the array in the example — and thus give the possibility of measuring some target property. Even incoherent addition of echoes suffers these difficulties and provides these opportunities. For example, if two FM pulses are transmitted, the difference between the times of arrival of the echoes will differ from the difference between their transmission times if the path length is changing. Since these time-difference changes may exceed the length of the matched filtered echoes, they must be taken into account by appropriately time shifting the first echo before adding it to the second; furthermore, in so doing, the rate of change of path length may be estimated.

The primary concern in this paper is with pairs of FM pulse echoes obtained either by transmitting pairs of pulses or receiving a single pulse on a pair of hydrophones. (Note that while in general a pair of hydrophones is talked about, in actual practice a pair of arrays — obtained for instance by using two arrays or using halves of a single array — would be used.) In this case how one echo must be modified to be coherent with the other can be determined by correlating suitably modified versions of the first echo with the second. For example, if the two echoes differ only by a time shift, then this time shift may be found by determining the peak of the time correlation between the two signals.

In the case of multiple FM echoes — obtained either by transmitting a pulse train or by receiving with an array of hydrophones — a different approach to coherent addition must be applied. In essence, this approach is nothing more than an extension of classical wide-band beam forming and it will be discussed in detail in a sequel document [2]. While the primary focus here is on FM pulses, many of the results are equally applicable to any broadband pulse such as a short CW pulse.

1 BACKGROUND

A significant effort over a long period of time has been spent at SACLANTCEN on the problem of detection and the extraction of measurements. No attempt will be made to give an exhaustive list of this work, which can be found in [3,4,5]; rather references will be made only to what seems most pertinent (some of those documents also contain extensive references ot previous works). One fact that distinguishes this work from previous work is that it is based on the theory presented by the author in [6]. In the first place, the use of this theory clears up some discrepancies in experimental results that will be discussed shortly and that were first resolved in [7]. In the second place, the use of this theory allows inclusion of true doppler effect rather than requiring use of the frequency-shift approximation to the doppler effect, which is inadequate for FM pulses used in modern matched-filter sonars.

Consider the matched-filter output for the echo from an FM pulse. From [6] the matched-filtered echo is a modified convolution in time shift τ and time stretch (doppler) α between the spreading function of the target and the ambiguity function of the pulse. The spreading function of a rigid narrow target may be represented as a line segment in the τ-α plane, as in shown in Fig. 1. The various measurement techniques to be described in this paper are aimed at eliciting properties of the target-spreading function, which are in

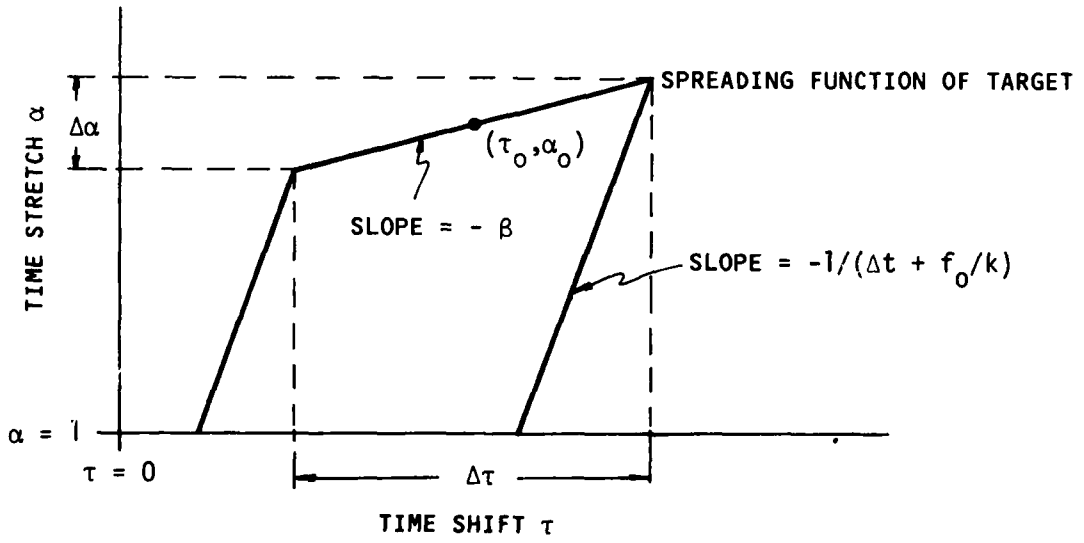

FIG. 1 MATCHED FILTER OUTPUT FOR FM PULSE AND LINE TARGET

turn closely related to target properties of interest. In particular, the

time shift τ_o and time stretch α_o of the centre of the spreading function of the target are related respectively to the path length ℓ between transmitter and receiver via the target at an arbitrarily defined zero time and to its rate of change $\dot{\ell}$ by

$$\tau_o = \ell/c \quad , \qquad 1-\alpha_o = \dot{\ell}/c \quad , \tag{Eq. 1}$$

where c is the speed of sound. (Note that in the monostatic case $\ell = 2r$ and $\dot{\ell} = 2\dot{r}$, where r is the range and $\dot{r}$ the range rate.) Furthermore, the spread of the spreading function in time shift $\Delta\tau$ is proportional to the apparent target length L', while its spread in time stretch $\Delta\alpha$ is proportional to the rate of change of apparent target length $\dot{L}'$:

$$\Delta\tau = 2L'/c \quad , \qquad \Delta\alpha = -2\dot{L}'/c \quad . \tag{Eq. 2}$$

(L' and $\dot{L}'$ will be defined in detail later; in the monostatic case they are $L\cos\alpha$ and $-\dot{\alpha}L\sin\alpha$ respectively, where L is the target length and α its aspect.) The slope of the target spreading function is β, where

$$\beta = -\dot{L}'/L \quad , \tag{Eq. 3}$$

and is closely related to the turning rate of the target. (In the monostatic case $\beta = \dot{\alpha}\tan\alpha$.)

From the results of [6], the effect of making a modified convolution with the ambiguity function of the FM pulse may be represented as projecting points in the τ-α plane onto the $\alpha=1$ axis by lines with slope $-1/(\Delta t_T + f_o/k)$, where Δt_T is the time of the FM transmission relative to the time for which the pulse would arrive at the target at $t = 0$; f_o is the centre frequency of the FM pulse and k is rate of change frequency in the pulse. This process is illustrated in Fig. 1 for the points on the ends of the target spreading function. This result makes intuitive sense, since the path length via a point with doppler α will change by $(1-\alpha)c\Delta t$ (see [6]) in time Δt, which corresponds to a change in delay of $(1-\alpha)\Delta t$; furthermore, the centre frequency of the pulse for this point will be shifted to αf_o, which corresponds to a time shift of $-(\alpha-1)f_o/k$ in the original pulse.

So far these results do not differ from the results that would be obtained had the frequency shift approximation to the doppler effect been used. In fact, however, a point on the spreading function does not project to a single point on the $\alpha = 1$ axis. Doppler has two major effects on an FM pulse, only the first of which appears in the frequency shift approximation: it shifts the centre frequency and it changes the slope in frequency; therefore, when a doppler-shifted FM pulse is passed through a filter matched to its original

form, energy is lost because the pass band of the filter does not match that of its input and the remaining energy is spread in time, both because the pass band is finite and because the individual frequency components of the input are not shifted by the appropriate phase. These two effects mean that both resolution and detection performance are degraded. In this paper the results of [6] are used to measure quantitatively the degradation in resolution and single-echo detection performance and also how measurement extraction performance is affected by the resolution obtainable.

The bandpass effect on resolution dominates for narrow-band FM signals while the slope effect dominates for large bandwidth signals. It is shown herein that there exists an optimum bandwidth for given centre frequency and pulse length that maximizes resolution for a given doppler shift. Kramer [8] has investigated the degradation of point-target detection caused by the diminuation of the peak matched-filter output resulting from slope mismatch. Herein both slope and bandpass mismatch are considered and it is shown that an optimum value of bandwidth exists for given centre frequency and pulse duration that maximizes peak matched filter output for a given doppler. For spread targets, on the other hand, the matched filter output will be averaged over an interval approximating the apparent length of the target [1]. In this case, it is shown herein that so long as the averaging interval exceeds the resolution interval of the pulse, increasing bandwidth improves detection performance because the fraction of energy lost is decreased.

Now consider measurement of target properties by use of a double FM pulse. The signal parameters of interest are the centre frequency f_{o_i}, rate of change of frequency k_i, duration T_i, and times Δt_{T_i} of the individual linear FM pulses, where the index $i = 1, 2$ is used to indicate the first and second pulse in the signal. Derived parameters of importance are the bandwidths $B_i = |k_i|T_i$ of the pulses, and the separation $\Delta T = \Delta t_{T_2} - \Delta t_{T_1}$ between the centres of the two pulses, $\Delta T' \triangleq (f_{o_1}/k_1 + f_{o_2}/k_2)$ and $\Delta T'' \triangleq (f_{o_2}/k_2 - f_{o_1}/k_1)$. In general the f_{o_i}'s and T_i's will be contrainted by other considerations, leaving the choice of the B_i's available for minimizing doppler dependence and minimizing measurement errors. In addition, the choice of ΔT and the signs of k_i strongly influence sensitivity of target-property measurements. (Given f_{o_i}, T_i and B_i, only the signs of k_i are free in determining $\Delta T'$ and $\Delta T''$.) The use of two identical pulses (for which $\Delta T'' = 0$) has the advantage that only one matched filter is required and disadvantage that it may be hard to distinguish which portion of the matched filter output corresponds to which FM pulse.

First consider what measurements can be obtained from incoherent processing of the echoes from two FM pulses — that is, matched filtering of the echoes, magnitude squaring the result, smoothing and measuring the length and delay of each echo. Figure 2 shows the matched filter output schematically for two FM pulses at times $\pm\Delta T/2$. Results are shown for the cases in which the first pulse is a down sweep $(k_1 < 0)$ and the second pulse is either a

downsweep chosen so that $\Delta T'' = 0$ $(f_{o_2}/k_2 = f_{o_1}/k_1)$ or it is an upsweep chosen so that $\Delta T' = 0$ $(f_{o_2}/k_2 = -f_{o_1}/k_1)$. A similar diagram can be drawn for an initial upsweep. Several results are immediately apparent from this diagram. If $\Delta T' = 0$ the average time shift of the centre of the two echoes is equal to τ_o and the average length in time of the two echoes is equal to $\Delta\tau$. Furthermore, the difference between the centres of the two echoes is $(1-\alpha_o)(\Delta T+\Delta T'')$ while the difference in lengths is $-\Delta\alpha(\Delta T+\Delta T'')$. Thus the sensitivity of these two measurements to (α_o-1) and $\Delta\alpha$ is $|\Delta T+\Delta T''|$, which is much greater when $\Delta T' = 0$, and is greatest when the down-up sequence is used since the effects of Δt_i and f_o/k_i then coincide; however this latter result is of minor significance since f_o/k_i is typically much larger than Δt_i.

Plaisant [9,10] proposed measuring the time shift of the centre and the length of a matched-filtered echo by finding the two time shifts at which the smoothed, matched-filtered echo power is at one-half its maximum value. The centre of the echo is then found by averaging these points and the length by differencing them. Furthermore, he developed equations for determining the standard deviation of the error in determining these half-power points by dividing the standard deviation of the smoothed power by the mean slope of the smoothed power at these points. Finally, he used these results to obtain equations for the standard deviations of the errors in measuring range, range rate, and apparent target length. Plaisant's results are extended in the present paper in several ways. In the first place, measurement of rate of change of apparent target length is considered and, in the second place the results are extended to the bistactic case in which range and range rate are replaced by path length and its rate of change. Furthermore, Plaisant uses the frequency shift approximation and considers only the case in which the resolution of the signal is greater than the smoothing interval, which in turn is small compared with the apparent target length (measured in time). These results are valid provided the resolution is determined using the time – stretch model of the doppler effect. In addition to this over-resolved case, the present paper also investigates the under-resolved case, in which the resolution of the pulses is less than the apparent target length but still greater than the smoothing interval (i.e. point targets) and also the cases of over- and under-resolved targets with no smoothing of the matched filter output.

Next, consider what measurements can be obtained from coherent processing of the echoes from two FM pulses: matched filtering of the echoes, correlating the two matched filter outputs in time and frequency, and determining the position in time and frequency shift of the peak in the magnitude of the correlation. Note that for this correlation to be possible, f_{o_1} and f_{o_2} must have almost the same value and hence may both be taken to be f_o. In analogy with incoherent processing, the time shift of the correlation peak is $(1-\alpha_o)(\Delta T+\Delta T''+\delta T)$, where δT is a correction proportional to the frequency shift of the peak. (This correction term, which cannot be neglected for large $|\beta|$, is found only with the time-stretch model of

doppler.) Furthermore, from Fig. 2 the second echo is stretched with respect to the first by

$$1-\beta\{(\Delta T+\Delta T")/[1+\beta(\Delta T/2-f_o/k_1)]\} \approx 1-\beta[\Delta T"/(1-\beta f_o/k_1)] \quad ,$$

since $\beta\Delta T$ is small compared with 1; therefore the two signals will lose correlation for large $|\beta|$ if $\Delta T'=0$ (and, hence, $\Delta T"$ is large). This result is shown herein by more detailed analysis and has been confirmed by unpublished sea trial results.

One might naively think that this same stretch acting on the carrier frequency would cause a corresponding frequency shift of the second echo with respect to the first and, hence, that the frequency shift of the correlation peak would be $\beta(\Delta T+\Delta T")f_o/(1-\beta\ f_o/k_1)$. In fact more careful analysis carried out herein and confirmed by unpublished sea trial results shows that — as first pointed out by the author in [7] — the frequency shift is just $\beta[\Delta T+(\alpha_o-1)\Delta T"]f_o/(1-\beta\ f_o/k_1) \approx \beta\ \Delta T\ f_o$.

Obviously use of $\Delta T"=0$ will cause little degradation in correlation with little loss in sensitivity of the frequency shift of the peak to β ; however, it will cause the sensitivity of the time shift of the peak to α_o-1 to be reduced greatly from $|\Delta T+\Delta T"|$ to $|\Delta T|$. To retain the sensitivity to α_o-1 and at the same time not degrade the correlation, more complex processing must be used in which the first matched-filtered echo is not only shifted in time and frequency, but also stretched to make it coherent with the second matched-filtered echo.

In the above analysis the ordinate of the spreading function is $\alpha = 1 - \frac{\partial \ell_p}{\partial t}\frac{1}{c}$, where ℓ_p is the path length via a given point; such a spreading function may be termed the temporal spreading function. For linear arrays there exists an analogous spreading function in which the ordinate is $\alpha_x = 1 - \frac{\partial \ell_p}{\partial x}$, where x is the distance along the array from an arbitrary origin; such a spreading function may be termed the spatial spreading function. (These two spreading functions are just two-dimensional projections of a three-dimensional spreading function whose independent variables are τ, α and α_x.) Targets at reasonable ranges and not too near end-fire will have a spatial spreading function that may be represented by a straight line segment in the τ-α_x plane and hence Fig. 1 applies with the ordinate α replaced by α_x. Corresponding to α and $\Delta\alpha$ are

$$\alpha_{x_o} = 1 + \cos\psi, \quad \Delta\alpha_x = -2\frac{\partial L'}{\partial x} \quad , \qquad \text{(Eq. 4)}$$

where ψ is target bearing relative to the array, since $\frac{\partial \ell}{\partial x} = -\cos\psi$. (In the monostatic case $\partial L'/\partial x = -L \sin\alpha \sin\psi/2r$, where r is the range from the origin of the array to the centre of the target). The slope of the spatial target spreading function is $c\ \beta_x$, where

$$\beta_x = -\frac{\partial L'}{\partial x} / L', \qquad \text{(Eq. 5)}$$

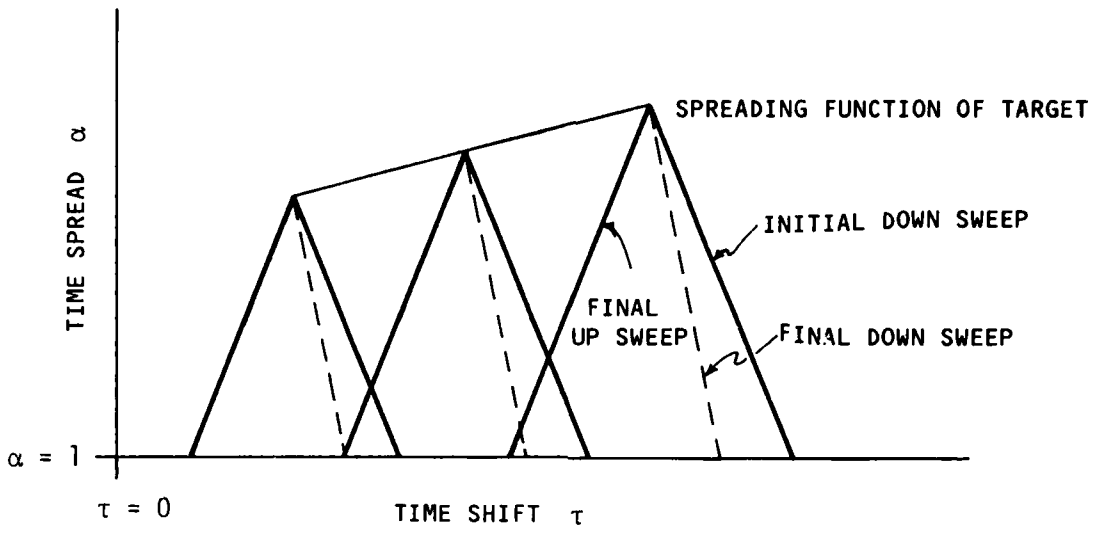

FIG. 2 MATCHED FILTER OUTPUT FOR DOUBLE FM PULSE AND LINE TARGET

and is closely related to the parallax of the target. (In the monostatic case $\beta_x = (\sin\psi/2r)\tan\alpha$ where $(\sin\psi/2r)$ is the parallax.)

In analogy with the temporal case, the matched filter output for a single echo from a motionless target heard by a single hydrophone located at Δx is a modified double convolution of the spatial spreading function with the spatial ambiguity function of the FM signal, which again may be represented as a projection onto the $\alpha_x = 1$ plane. Figure 1 again applies, with α replaced by α_x and the slope of the projection equal to $-c/x$. For a moving target three dimensions are required, with the output of the matched filter being a double projection onto the $\alpha=\alpha_x=1$ line. If two hydrophones at $x = \pm\Delta x/2$ are used, Fig. 2 applies, with the line labelled "initial downsweep" applying for the hydrophone at $-\Delta x/2$ and that labelled "final-upsweep" applying for the hydrophone at $\Delta x/2$. In analogy with the temporal results, α_{x_o} and β_x may be measured by correlating the matched filter outputs from the two hydrophones in time and frequency. The time and frequency shift of the peak magnitude of correlation are, analogously, $(1-\alpha_{x_o})\Delta x+(1-\alpha_o)\delta T_x$ (where δT_x is a correction proportional to the frequency shift of the peak) and $\beta_x \Delta x f_o/(1-\beta f_o/k)$.

Wiekhorst *[11]* was the first to suggest measurement of the target aspect using the frequency difference between the echoes received at two hydrophones — a technique he referred to as space/frequency. In analogy, Seynaeve and van Marle *[12]* proposed using two pulse separated in time to measure apparent turning rate. (In this paper — as has already been done — the analogy is used in the reverse direction from temporal to spatial processing.) Subsequent to Wiekhorst's original study much effort was expended at SACLANTCEN on these techniques, most of which involved use of the envelopes of the echoes rather than matched-filter outputs. (The envelopes of the echo from a linear FM is an approximation to the frequency response of the target expressed as a function of time, while from *[6]* — see below — the fourier transform of the matched-filter output is also a measure of the frequency response of the target.) This procedure had the advantage of easing computer requirements — an advantage of great importance at the time the work was carried out, but of little importance now. It suffered the major defect that the frequency shift between the echoes was shifted into the time domain hence making it impossible to separate the effects of α_o-1 or $\alpha_{x_o}-1$ from those of β or β_x. Hug *[13]* first suggested use of matched filters and correlation in time and frequency to obviate this problem in spatial processing. He *[14]* and Plaisant *[9,10]* made further studies of the use of the double correlation approach in temporal processing.

Plaisant proposed finding the frequency shift of the correlation peak using the same technique that he proposed for incoherent processing: namely, to find the frequency shifts at which the correlation peak falls to one half its peak value and average them. Furthermore, he derived expressions for the standard deviation of the error in β by using his previous technique of dividing standard deviation by mean slope to determine the error standard deviation for measuring the two half-peak frequency shifts. His

results are extended in the present paper to measurement of the time shift of the correlation peak and determination of its error standard deviation. Also treated is the use of the phase of the correlation peak to improve the estimate of the time shift between the two echoes. This process is in effect an updated version of split-beam processing. Wiekhorst in his original work suggested using a double FM pulse as well as two hydrophones with incoherent processing between the echoes from the two pulses in addition to coherent processing between the two hydrophones for each pulse. In addition to investigating this approach and determining the corresponding measurement error standard deviations using Plaisant's approach, the present paper also treats the use of coherent temporal as well as spatial processing for a two-hydrophone, two-pulse combination.

One final topic must be covered before concluding this background. Figure 1 shows pictorally how the matched-filtered echo from a moving, turning, line target for a linear FM pulse in a non-dispersive medium is related to the spreading function of such a target. In *[6]* there is a detailed derivation of the matched filter output $\phi^D(\tau,1)$ that will serve as the basis of the detailed analysis contained in the body of this paper. With noise added to the noise-free result of *[6]* and the subscript i added to distinguish the first and second pulse, we have

$$\phi_i^D(\tau,1) = e^{2\pi j\, f'_{o_i}(\tau-\tau'_{d_i})}\, \psi_i^M(\tau-\tau_{d_i}) + n_i(\tau)\ , \qquad \text{(Eq. 6)}$$

where $n(\tau)$, is noise, the delays τ'_{d_i} and τ_{d_i} depend on target properties, and the shifted carrier frequency f'_{o_i} depends on f_o and target properties. The modulation in turn may be expressed in the time domain as the convolution of a resolution function $\gamma^M_{FM_i}$ and an impulse response h_i^M or in the frequency domain as the product of a window function $\Gamma^M_{FM_i}$ and a transfer function H_i^M :

$$\psi_i^M(\tau) = \int_{-\infty}^{\infty} \gamma^M_{FM_i}(\tau-\tau',\, \alpha_o)\, h_i^M(\tau')d\tau,$$

$$\Psi_i^M(f) = \Gamma^M_{FM}(f,\, \alpha_o)\, H_i^M(f). \qquad \text{(Eq. 7)}$$

The modulation function and the window function, which are fourier transform pairs, represent the properties of the pulse, while the impulse response and transfer function, which are also fourier transform pairs, represent the properties of the target. Note, therefore, that a measure of the frequency response of the target is obtained by fourier transforming the matched-filter output.

The organization of the present paper is as follows: first to be discussed are the resolution and single-echo detection capability of a linear FM pulse. Next are the incoherent and coherent measurements of target properties using a double FM pulse. Third are space/frequency measurements using a pair of hydrophones and a double FM pulse. The final topic is how all these results can be used in practical algorithms.

2 RESOLUTION

This chapter is concerned with the spread of $|\gamma^M_{FM_i}|^2$ in τ as a function of f_{o_i}, T_i, B_i and α_{o_i}. It is convenient to drop the indices and use the normalized variables defined in *[6]* whose definitions are repeated here (with α replaced α_o) for convenience

$$x = kT\sqrt{T/f_o}/\alpha_o \approx kT\sqrt{T/f_o},$$

$$y = (\alpha_o - 1)\sqrt{f_o T}/\alpha_o \approx (\alpha_o - 1)\sqrt{f_o T}, \qquad \text{(Eq. 8)}$$

$$v = \alpha_o/\sqrt{f_o T} \approx 1/\sqrt{f_o T},$$

$$z = kT\tau .$$

It was shown in *[6]* that in most sonar situations we may use v=0 in expressions for γ^M_{FM} – a practice that will be followed throughout this document. In that case, from *[6]* it follows that $|\gamma^M_{FM}|^2$ is independent of the sign of x and y; hence they may be replaced by $|x| \approx B\sqrt{T/f_o}$ and $|y| \approx |\alpha_o - 1|\sqrt{f_o T}$. To determine the resolution of $|\gamma^M_{FM}|^2$ a measure of its spread is required. One such measure is the difference between the smallest and largest value of z at which $|\gamma^M_{FM}|^2$ is some fraction of the peak value of $|\gamma^M_{FM}|^2$ over z. In terms of τ the spread is, from Eq. 8, $1/B$ times smaller. Since the spread in terms of τ is the quantity of interest this will be termed the resolution, while the spread in z divided by $|x|$ will be termed the normalized resolution. Note that the normalized resolution is $\sqrt{f_o/T}$ times the ordinary resolution.

If the fraction defining the spread in z or τ is taken to be $4/\pi^2 \approx 0.4$, it is well known that for no doppler the resolution (in this case the difference between the minimum and maximum τ at which

$$|\gamma^M_{FM}|^2 = [\mathrm{sinc}(\pi B\tau)]^2 = 4/\pi^2, \text{ i.e. } \tau = \pm 0.5/B)$$

is 1/B and the corresponding normalized resolution is just $1/|x|$. For small $|xy|$ it was shown in *[6]*, that $|\gamma^M_{FM}|^2$ is stretched by the factor $1/(1-|y/x|)$; hence the normalized resolution is $1/(|x|-|y|)$. On the other hand, it was also shown in *[6]* that, for large $|x, y|$, $|\gamma^M_{FM}|^2$ is rectangular, with width $2|yx|(1-|y/x|)$; hence the normalized resolution is $2|y/x|(|x|-|y|)$. The former function decreases with $|x|$ for given $|y|$, while the latter increases with $|x|$ for given $|y|$; therefore a possible approximation to the normalized resolution is the maximum of these two functions. Unfortunately this approximation is not adequate near the best resolution, as may be seen from Fig. 3, which plots the actual normalized resolution and this approximation to it as a function of $|x|$ for $|y| = 0.84$. (For f_o=3500 Hz and T=0.5 s this $|y|$ corresponds to $|\alpha_o - 1| = |\dot{\ell}/c| = 0.02$, which thus corresponds to $|\dot{\ell}| = 60$ kn or $|\dot{r}| = 30$ kn in the monostatic case and, hence, is a reasonable upper bound on $|\alpha_o - 1|$ as was pointed out in *[6]*.)

The problem with the approximation just discussed is the inadequacy of the large $|xy|$ approximation. In Appendix A a more suitable approximation to the spread for large $|xy|$ is derived that is valid for smaller $|xy|$. It is $|x| / \{(|x|-|y|)(1- \sqrt{1-|x| / [(|x|-|y|)^2|y|]})\}$ and it reduces to the above approximation when $|xy|$ is sufficiently large. The corresponding resolution is just this function divided by $|x|$. A second possible approximation to the normalized resolution is the maximum of the previously-given small $|xy|$ approximation and this new large $|xy|$ approximation. Fortunately, as may be seen from Fig. 3, this approximation is more than adequate — especially since the definition of resolution is somewhat fuzzy in any case.

The minimum spread (corresponding to maximum resolution) occurs when the small and large $|xy|$ approximations are equal; this equality occurs when the square root in the large $|xy|$ approximation is zero — that is for $|x| = x^*$ where

$$(x^*)^2 - 2|y| \; x^* + |y|^2 = \frac{x^*}{|y|}$$

or — since the largest root is obviously the required one — when

$$x^* = |y| + 1/(2|y|) + \sqrt{1 + 1/(4|y|^2)} \; . \qquad \text{(Eq. 9a)}$$

In terms of the original variables this result implies that the optimum bandwidth is

$$B^* \approx |\alpha_o - 1| \; f_o + 1/(2|\alpha_o - 1|T) + \sqrt{f_o/T + 1/(2|\alpha_o - 1|T)^2} . \qquad \text{(Eq. 9b)}$$

Since for any fixed B the spread of $|\gamma^M_{FM}|^2$ in τ increases with $|\alpha_o - 1|$, it follows that the B^* corresponding to the largest $|\alpha_o - 1|$ of interest should be used.

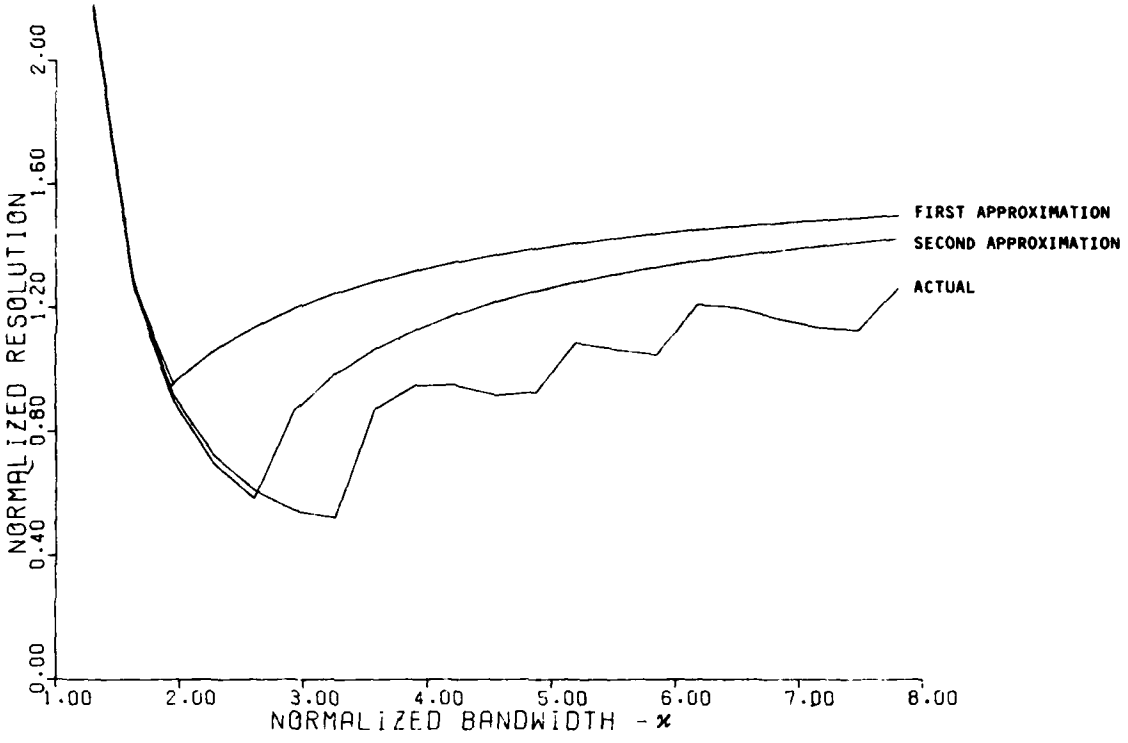

FIG. 3 RESOLUTION FOR $y = 0.84$

The normalized resolution corresponding to x* is

$$2|y| \;/\; (1 + \sqrt{4|y|^2 + 1}) \qquad \text{(Eq. 10a)}$$

and the corresponding ordinary resolution corresponding to B^* is

$$2|\alpha_o - 1|T \;/\; (1 + \sqrt{1 + 4(\alpha_o - 1)^2 f_o T}). \qquad \text{(Eq. 10b)}$$

For $|x| > x^*$ the spread of $|\gamma^M_{FM}|^2$ increases slowly; in fact it reaches its maximum at $|x|=\infty$, for which the maximum normalized resolution is $2|y|$. The corresponding ordinary resolution at $B=\infty$ is $2|\alpha_o - 1|T$. On the other hand, for $|x|<x^*$ the spread of $|\gamma^M_{FM}|^2$ increases rapidly; the normalized resolution is $2|y|$ for $|x| = |y| + 1/2|y|$. Correspondingly, the ordinary resolution $2|\alpha_o - 1|T$ occurs for $B = |\alpha_o - 1| f_o + 1/(2|\alpha_o - 1|T)$. For example, for f_o = 3500 Hz, T = 0.5 s and $|\alpha_o - 1|$ = 0.02, B^* = 217 Hz and the corresponding resolution is 6.8 ms — not much worse than the 4.6 ms resolution for zero doppler. Furthermore the resolution is 20 ms at B = 120 Hz and B = ∞ Hz.

3 SINGLE-ECHO DETECTION

The detection of point targets is first considered, followed by a consideration of the detection of distributed targets. As in the previous chapter, the subscript i will be dropped throughout.

3.1 Point Targets

Optimum detection of point targets is based on comparisons of the output power of the matched filter with a threshold. In this case the signal power in the matched filter output is $|\gamma^D_{FM}|^2$; therefore the key quantity of interest is the maximum of $|\gamma^D_{FM}|^2$. Thus this section is concerned with how this maximum varies with doppler and how FM signal parameters should be chosen to minimize its falloff with increasing doppler. For this purpose we make the somewhat arbitrary assumption that we can tolerate a falloff in the maximum of $|\gamma^D_{FM}|^2$ to one half of its maximum at no doppler, which is $|\gamma^D_{FM}(0,0)|^2 = 1$. Again it is convenient to use the normalized variables defined in Eq. 8.

From *[6]* it is apparent that for fixed α_o the maximum of $|\gamma^M_{FM}|^2$ over z occurs near z=0 (at least for peaks of reasonable magnitude), and, furthermore, $|\gamma^M_{FM}|^2$ is independent of v and an even function of x and y for z=0; hence the only remaining variables are |x| and |y|. Let y*(|x|) be

the value of $|y|$ that for given $|x|$ yields $|\gamma^M_{FM}(0,\alpha_o)|^2 \approx 0.5$. Since α_o is very close to 1, by the above criterion, we seek the value of $|x|$ for which $y^*(x)$ is maximized. Figure 4 is a plot of y^* against $|x|$, from which it is apparent that this value of $|x|$ is $|x| = 2.6$, for which $y^* \approx 0.58$. (A discussion of how Fig. 4 was generated is contained in Appendix B.) In terms of the original variables the above result implies that to optimize point-target detection B should be close to

$$B^\dagger = 2.6 \sqrt{f_o/T}, \qquad \text{(Eq. 11)}$$

and that the corresponding maximum doppler is

$$\alpha^\dagger = 1 \pm 0.58 / \sqrt{f_o/T}. \qquad \text{(Eq. 12)}$$

If $f_o = 3500$ Hz and $T = 0.5$ s, $B^\dagger = 218$ Hz and $|\alpha_o - 1| = 0.014$, which corresponds to $|\dot{\ell}| = 42$ kn or in the monostatic case $|\dot{r}| = 21$ kn.

3.2 Distributed Targets

Generally the resolution of the pulses will be sufficient to over-resolve the target. In this case point-target estimation is not optimal and a detector very close to the optimum may be obtained by averaging the matched-filter output power over an interval before comparing it with a threshold (see Heering *[1]*). The length of the interval, which is not critical, should approximate the target length in time. If the target is a line target and the scatterers are uncorrelated at separations larger than the width of $|\gamma^M_{FM}|^2$ in τ, Eqs. 6 and 7 imply that the echo power after integration is the convolution in τ of a function representing the target with $|\gamma^M_{FM}|^2$, followed in turn by the convolution of the result with the averaging interval. Since the convolution operator is associative, this process is equivalent to convolving $|\gamma^M_{FM}|^2$ with the averaging integral, followed by convolution of the result with the function representing the target. Thus in this case the total energy, rather than the maximum power, of γ^M_{FM} is of interest – provided γ^D_{FM} has sufficient resolution (i.e. is sufficiently narrow) that most of its energy is contained within a time interval smaller than the averaging interval.

Now the total energy in γ^M_{FM} is by definition the integral $|\gamma^M_{FM}|^2$ over all τ (or equivalently all z). But by Parsival's relationship the integral of $|\gamma^M_{FM}|^2$ over z equals the integral of $|\Gamma^M_{FM}|^2$ over the normalized frequency $w = f/B$. Under the assumption that the approximation $v = 0$ is valid, from *[6]*

$$|\Gamma^M_{FM}(w,y)|^2 \approx \sqcap(y/x;1)\sqcap(2w;1-|y/x|); \qquad \text{(Eq. 13)}$$

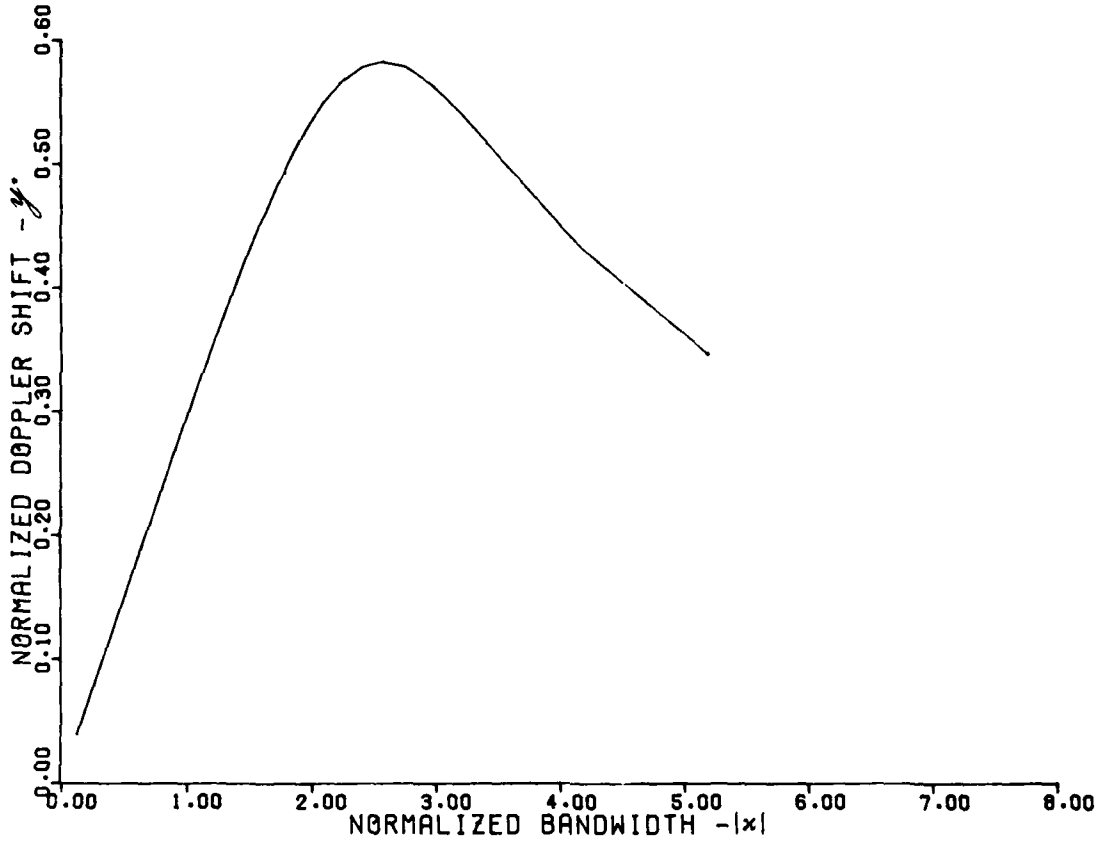
NORMALIZED DOPPLER SHIFT - y*
0.00
0.10
0.20
0.30
0.40
0.50
0.60
0.00
1.00
2.00
3.00
4.00
5.00
6.00
7.00
8.00
NORMALIZED BANDWIDTH -|x|

FIG. 4 y^* vs $|x|$

therefore

$$\int_{-\infty}^{\infty} |\gamma_{FM}^{M}|^2 \, dz = \int_{-\infty}^{\infty} |\Gamma_{FM}^{M}|^2 \, dw = \curvearrowright(y/x;1) \, (1 - |\tfrac{y}{x}|) \; . \qquad \text{(Eq. 14)}$$

If $y^*(|x|)$ is selected to make the integral in Eq. 14 fall to 0.5, as was done before with the maximum, it is clear that $y^* = 0.5|x|$. In terms of the original variables, this result implies that detection performance can be made as large as desired by increasing B – provided that the integration interval is large enough. The corresponding maximum doppler is

$$|\alpha_o - 1| = 0.5 \; B/f_o \; . \qquad \text{(Eq. 15)}$$

For example, if f_o = 3500 Hz, T = 0.5 s and B = 217 Hz, this result corresponds to $|\dot{\ell}| \leq 93$ or, in the monostatic case, $|\dot{r}| < 46.5$ kn. For this case we have previously seen that for $|\alpha_o - 1| < 0.02$, the resolution is 6.8 ms or better. This is much smaller than a typical integration interval of 50 to 100 ms. Furthermore, note that if $|\alpha_o - 1| < 0.02$, the total energy in $|\gamma_{FM}^{M}|^2$ over τ falls only 32% (or 1.7 dB) from the maximum value at maximum doppler.

4 INCOHERENT MEASUREMENTS

Now consider measurement of target properties – this chapter will treat incoherent techniques and the next will treat coherent techniques. First, the measurement of target properties is reduced to an estimation of the time shifts and of the spread of the modulation of the matched filter outputs. Second, the use of Plaisant's approach *[9,10]* to estimate these quantities is studied. Third, the standard deviation and correlations of the errors in measuring target properties are related to the like properties of estimation errors for the modulation time shifts and spreads. Finally, consideration is given to the selection of appropriate signal and signal-processing parameters.

4.1 Basic measurement principle

Since most of the target properties of interest are time-varying, a time of measurement must be specified. The most convenient time is that at which the centre of the signal arrives at the target. The delay of the modulation of the matched filter output for the echo from the ith FM pulse is, from *[6]*,

$$\tau_{d_i} = [\ell + \frac{c\dot{\ell}}{c-\dot{\ell}} \, (\Delta t_{T_i} + f_{o_i}/k_i)]/c \; ,$$

$$\approx [\ell + \dot{\ell} \, (\Delta t_{T_i} + f_{o_i}/k_i)]/c \; ; \qquad \text{(Eq. 16)}$$

If τ_{d_i} can be estimated -- say by $\tilde{\tau}_{d_i}$ — then ℓ and $\dot{\ell}$ can be estimated respectively,

$$\tilde{\ell} = (\tilde{\tau}_{d_1} + \tilde{\tau}_{d_2})\, c/2 - \tilde{\dot{\ell}}\Delta T'/2$$

$$\tilde{\dot{\ell}} = (\tilde{\tau}_{d_2} - \tilde{\tau}_{d_1})\, c/(\Delta T + \Delta T''), \qquad \text{(Eq. 17)}$$

if, as is assumed from now on, $\Delta t_{T_2} = -\Delta t_{T_1} = \Delta T/2$.

As in *[9,10]* the target is modelled herein as a time segment of uncorrelated scatterers of length L ; therefore, from *[6]*, $h_i^M(\tau)$ is a segment of white noise of length

$$\Delta\tau_{d_i} = 2L' \left[1 + \frac{c^2\dot{L}'}{(c-\ell)^2}(\Delta t_{T_i} + f_{o_i}/k_i) - a\right]/c$$

$$\approx 2L' \left[1 + \dot{L}'(\Delta t_{T_i} + f_{o_i}/k_i)\right]/c \ . \qquad \text{(Eq. 18)}$$

The apparent length L' , its rate of change $\dot{L}'$ and a are defined by:

$$L' = L[\cos\alpha + \cos(\alpha-\gamma)]/2,$$

$$\dot{L}' = L[\dot{\alpha}\sin\alpha + (\dot{\alpha}-\dot{\gamma})\sin(\alpha-\gamma)]/2,$$

$$a = \dot{\ell}\, L\cos\alpha/2L' \ , \qquad \text{(Eq. 19)}$$

where α is the target aspect, γ is the bistatic angle, and $\dot{\alpha}$ and $\dot{\gamma}$ are the rates of change of α and γ — all evaluated at $t = 0$. If $\Delta\tau_{d_i}$ can be estimated — say by $\Delta\tilde{\tau}_{d_i}$ — then L' and $\dot{L}'$ may be estimated by

$$\tilde{L}' = (\Delta\tilde{\tau}_{d_2} + \Delta\tilde{\tau}_{d_1})c/4 - \tilde{\dot{L}}'\,\Delta T'/2 \ ,$$

$$\tilde{\dot{L}}' = (\Delta\tilde{\tau}_{d_2} - \Delta\tilde{\tau}_{d_1})\, c/[2(\Delta T + \Delta T'')]. \qquad \text{(Eq. 20)}$$

4.2 Plaisant's approach to estimation of modulation delays and spreads

Now consider estimation of τ_{d_i} and $\Delta\tau_{d_i}$. Plaisant *[9,10]* developed the following technique: The power in the matched-filter output is smoothed by taking a moving average over a suitable interval. For each echo the echo plus noise and noise levels in the smoothed, matched-filter output are estimated and the beginning and end of the echo estimated by seeing where the smoothed echo power crosses a threshold level corresponding to the average of these two levels. Finally τ_{d_i} is estimated as the average of the beginning and end of the echo while $\Delta\tau_{d_i}$ is estimated as the difference between the beginning and end of the echo. Plaisant does not discuss how the echo plus noise and noise levels are to be determined; some approaches will be discussed later, for the moment it is assumed that errors in determining these levels are negligible. Clearly the average of the two levels is one half the echo level in the smoothed matched-filter output; hence the two points for which the smoothed echo power cross the threshold levels will be referred to as the half-echo-power points.

Two types of errors may occur in the determination of the half-echo-power points: global errors and local errors. A global error occurs when noise alone exceeds the threshold level (see *[9]*, pp 13 to 16). A basic purpose of smoothing the matched filter output power is to decrease the probability of global errors. If a threshold on echo signal-to-noise ratio (estimated from the echo-plus-noise and noise levels) is set and only those echoes whose signal-to-noise ratio exceed the threshold are selected for measuring target properties, the probability of global error can be minimized. On the other hand, local errors occur because of the variation of the smoothed matched-filter power about its expected value. In the remainder of this section the standard deviation of such errors will be considered in more detail. In general, the standard deviation of the local error in measuring a half-echo-power points will be found, as Plaisant *[9,10]* did, by dividing the standard deviation of the smoothed matched filter power at the half-echo-power points by the slope of the expected smoothed matched-filter power at these points.

From Eqs. 6 and 7 the expected value of the smoothed matched-filter power $P_i(\tau)$ is

$$P_i(\tau) = \frac{1}{T_{S_i}} \sqcap(\tau;T_{S_i}/2) \underset{\tau}{\circledast} |\gamma^M_{FM_i}(\tau,\alpha_o)|^2 \underset{\tau}{\circledast} \frac{1}{\Delta\tau_{d_i}} \sqcap(\tau-\tau_{d_i};\Delta\tau_{d_i}/2)\sigma_{e_i}{}^2 + \sigma_n{}^2 \qquad \text{(Eq. 21)}$$

where T_{s_i} is the smoothing interval, $\sigma_{e_i}{}^2$ is the echo energy, $\sigma_n{}^2$ is the noise power density (assumed flat over the frequency band of interest), and $\underset{\tau}{\circledast}$ is convolution in τ. Note immediately from this equation that $\Delta\tau_{d_i}$ cannot be measured if it is less than T_{s_i}.

Plaisant implicitly assumes that the spread of $|\gamma^{M}_{FM}(\tau,\alpha_o)|$ is small compared with the minimum of T_{s_i} and $\Delta\tau_{d_i}$; i.e. its resolution is greater than they are. For the moment we assume that this is true. The smoothed matched-filter output power contains echo and noise. For no doppler, the noise and echo were modelled by Plaisant, and are modelled herein, by gaussian white noise passed through a filter of bandwidth B_i; hence the standard deviation of the smoothed power at the half-power point can be readily calculated. For a non-zero doppler the echo is no longer white noise passed through a filter of bandwith B_i, but rather through a filter of bandwidth $B_i - |\alpha_o - 1| f_{o_i}$, because of the frequency shift caused by the doppler effect. (For this situation the stretch about the centre frequency may be neglected.) The result is that Plaisant's equation for the standard deviation in measurement of the time of a half-power point must be modified to

$$\sigma_{\tau_i} = T_i^* \sqrt{\frac{1}{B_i T_{s_i}}} \sqrt{\frac{B_i\, T_{s_i}}{2(B_i - |\alpha_o - 1| f_{o_i}) T_i^*} + \frac{1}{S/N_i} + \frac{1}{(S/N_i)^2}} \quad , \qquad \text{(Eq. 22)}$$

where

$$T_i^* = \min[T_{s_i}, \Delta\tau_{d_i}] \, ,$$

$$S/N_i = \sigma_{e_i}^2 (B_i - |\alpha_o - 1| f_{o_i})\, T_i^* / (\sigma_n^2\, B_i^2\, \Delta\tau_{d_i}\, T_{s_i})$$

(Note S/N_i is the smoothed power signal-to-noise ratio.)

A derivation of this result is contained in Appendix C*.

Now suppose that the spread of $|\gamma^{M}_{FM_i}(\tau,\alpha_o)|$ is still small compared with T_{s_i} but not with respect to $\Delta\tau_{d_i}$. In fact, suppose that $\Delta\tau_{d_i}$ is sufficiently small that $\sqcap\!\!\sqcup\,(\tau-\tau_{d_i}\,;\,\Delta\tau_{d_i}/2)/\Delta\tau_{d_i}$ may be considered to be a δ function in Eq. 21. In this case — following Plaisant's analysis of LCW measurement with a non-turning target — the variation in smoothed

---

*Note that in Plaisant's work *[9,10]* $\sigma_{e_i}^2$ and σ_n^2 are noise powers rather than energy and noise power density, respectively, as herein; thus the extra factor $B_i \Delta\tau_{d_i}$ in the denominator of S/N_i.

output power is assumed to be caused by noise alone. The result is

$$\sigma_{\tau_i} = \frac{(B_i - |\alpha_o - 1| f_{o_i})}{B_i^2 |\gamma^M_{FM_i}(0,\alpha_o)|^2} \sqrt{\frac{1}{B_i T_{s_i}}} \frac{1}{S/N_i} \quad . \qquad \text{(Eq. 23)}$$

As with Eq. 22, a derivation of this result is contained in Appendix C. Determining σ_{τ_i} for $\Delta\tau_{d_i}$ roughly equal to the spread of $|\gamma^M_{FM_i}(\tau,\alpha_o)|^2$ – i.e. the transition between Eqs. 22 and 23 as $\Delta\tau_{d_i}$ becomes progressively smaller – is much more difficult and will not be done herein. Note that the factor before the square root in Eq. 23 is the area under $|\gamma^M_{FM_i}(\tau,\alpha_{oi})|^2$ divided by its height at $\tau = 0$ and hence a measure of its spread; therefore this factor is consistent with the first factor in Eq. 22, which is also a spread.

Finally consider the modifications required to Eqs. 22 and 23 as T_{s_i} becomes smaller and smaller. For T_{s_i} of the order of the spread of $|\gamma^M_{FM_i}(\tau,\alpha_o)|^2$, the situation is too complicated to be treated herein.

For T_{s_i} less than $1/B_i$, which is certainly less than the spread of $|\gamma^M_{FM_i}(\tau,\alpha_o)|^2$, there is no smoothing of either signal or noise; therefore the moving average may be dispensed with – that is T_{s_i} set to zero. In this case, for $\Delta\tau_{d_i}$ greater than the spread of $|\gamma^M_{FM_i}|^2$, the variation in the power (unsmoothed now) at the half-echo-power points has a chi-squared distribution with a mean equal to the noise power plus one half the echo power; as a result

$$\sigma_{\tau_i} = \frac{B_i - |\alpha_o - 1|\ f_{o_i}}{B_i^2 |\gamma^M_{FM_i}(0,\alpha_o)|^2} \sqrt{\frac{1}{4}\frac{1}{S/N_i} + \frac{1}{(S/N_i)^2}} \qquad \text{(Eq. 24)}$$

Note that Eq. 24 retains the same form as Eqs. 22 and 23 except that $B_i T_{s_i}$ is now replaced by unity. For $\Delta\tau_{d_i}$ less than the spread of $|\gamma^M_{FM_i}(\tau,\alpha_o)|^2$ only the noise power contributes to the variation and the result is

$$\sigma_{\tau_i} = \left[|\gamma^M_{FM_i}(0,\alpha_o)|^2 \Big/ \frac{\partial |\gamma^M_{FM_i}(\tau_i^*,\alpha_o)|^2}{\partial\tau} \right] \left(\frac{1}{S/N_i}\right) \qquad \text{(Eq. 25)}$$

where $\tau_i^* < 0$,

$$|\gamma^M_{FM_i}(\tau_i^*,\alpha_o)|^2 = \frac{1}{2}|\gamma^M_{FM_i}(0,\alpha_o)|^2 ,$$

$$S/N'_i = \sigma_{e_i}{}^2 |\gamma^M_{FM_i}(0,\alpha_o)|^2/\sigma_n{}^2 .$$

As before, detailed derivations of Eqs. 24 and 25 are given in Appendix C.

These results are for the noise-limited case. In the reverberation-limited case – provided that the reverberation power is constant over an interval of length equal to the greatest of T_s, $\Delta\tau_d$ and the spread of $|\gamma^M_{FM_i}|^2$ and that the spread in doppler of the reverberation is modest (both good approximations) – the reverberation can be treated as a zero doppler, non-turning target of infinite extent. In this case reverberation acts like a noise of power density $\sigma_r{}^2/B_i$, where $\sigma_r{}^2$ is the expected reverberation power; therefore all the previous equations are valid for the reverberation-limited case provided that $\sigma_n{}^2$ is replaced by $\sigma_r{}^2/B_i$ in the equations for S/N_i and S/N'_i . In the remainder of this paper, although only the noise-limited case is referred to, it is to be understood that the reverberation-limited case can be treated by this artifice. Obviously $B_i = \sigma_r{}^2/\sigma_n{}^2$ is the breakpoint between the noise-and reverberation-limited cases, with the noise-limited case applying for B_i greater than this value. Note that from Eq. 22 S/N_i is increasing with B_i for the reverberation-limited case and decreasing with B_i for the noise-limited case, hence the maximum S/N_i is obtained for $B_i = \sigma_r{}^2/\sigma_n{}^2$; similar comments apply to S/N'_i .

As stated earlier, these results are based on the assumption that the target is a line segment of independent reflectors whose amplitude have identical gaussian distributions. In fact there is evidence that a better model of a submarine is obtained if the gaussian distribution is replaced by a double-gaussian distribution – i.e. the amplitude is chosen, with given probabilities, from one of the two gaussian distributions *[15]*. This model is consistent with the view what the submarine consists of numerous small amplitude reflectors plus a small number of highlights. A major difference between the gaussian and double-gaussian distributions is that for the same expected echo powers the variance in echo power will be greater with the double gaussian. Thus if the gaussian hypothesis is replaced by a double-gaussian hypothesis in the analysis leading to Eqs. 22 and 24, the result will be to increase the magnitude of the first terms under the final square root. Similar considerations will apply to the coherent processing discussed in the next chapter.

Given expressions for the standard deviation in the estimation of the echo-half-power points σ_{τ_i}, the standard deviations $\sigma_{\tau_{d_i}}$ and $\sigma_{\Delta\tau_{d_i}}$ of the estimates $\tilde{\tau}_{d_i}$ and $\Delta\tilde{\tau}_{d_i}$ found by taking the average of and the difference between the estimated half-echo-power points, are – assuming no correlation between the estimated half-echo-power points –

$$\sigma_{\tau_{d_i}} = \sigma_{\tau_i} / \sqrt{2} \quad , \qquad \sigma_{\Delta\tau_{d_i}} = \sigma_{\tau_i} \sqrt{2} \quad . \qquad \text{(Eq. 26)}$$

The errors in the estimated $\tilde{\tau}_{d_i}$ and $\Delta\tilde{\tau}_{d_i}$ are uncorrelated since the sum and difference of two uncorrelated variables with the same standard deviation are uncorrelated.

4.3 Standard deviations and means of the measurement errors

Given any technique for estimating τ_{d_i} and $\Delta\tau_{d_i}$ – such as the approach of Plaisant just covered – then the second-order statistical properties of the estimates $\tilde{\ell}$, $\dot{\tilde{\ell}}$, $\tilde{L}'$ and $\dot{\tilde{L}}'$ are readily obtainable from $\sigma_{\tau_{d_i}}$, $\sigma_{\Delta\tau_{d_i}}$ and $\rho_{\tau_{d_i}\Delta\tau_{d_i}}$ – the correlation between the errors in $\tilde{\tau}_{d_i}$ and $\Delta\tilde{\tau}_{d_i}$ – by the use of Eqs. 17 and 20. For simplicity, we assume, as is typically true, that $\sigma_{\tau_{d_i}} = \sigma_{\tau_{d_2}} = \sigma_{\tau_d}$ and $\sigma_{\Delta\tau_{d_1}} = \sigma_{\Delta\tau_{d_2}} = \sigma_{\Delta\tau_d}$; then the standard deviations of the estimates are, by inspection, respectively

$$\sigma_{\tilde{\ell}} = \sigma_{\tau_d} c \sqrt{\{1 + [\Delta T'/(\Delta T+\Delta T")]^2\}/2} \quad ,$$

$$\sigma_{\dot{\tilde{\ell}}} = \sigma_{\tau_d} c \sqrt{2}/|\Delta T+\Delta T"| \quad ,$$

$$\sigma_{\tilde{L}'} = \sigma_{\Delta\tau_d} c \sqrt{\{1 + [\Delta T'/(\Delta T+\Delta T")]^2\}/8} \quad ,$$

$$\sigma_{\dot{\tilde{L}}'} = \sigma_{\Delta\tau_d} c /(\sqrt{2}|\Delta T+\Delta T"|) \quad . \qquad \text{(Eq. 27)}$$

Furthermore, the correlations between $\tilde{\ell}$ and $\dot{\tilde{\ell}}$ and between $\tilde{L}$ and $\dot{\tilde{L}}$ are

$$\rho_{\tilde{\ell}\dot{\tilde{\ell}}} = \Delta T' \sigma_{\dot{\tilde{\ell}}}/(2 \sigma_{\tilde{\ell}}) \quad ,$$

$$\rho_{\tilde{L}\dot{\tilde{L}}} = \Delta T' \sigma_{\dot{\tilde{L}}'}/(2 \sigma_{\tilde{L}'}) \quad . \qquad \text{(Eq. 28)}$$

Finally if $\rho_{\tau_{d_i}\,\Delta\tau_{d_i}}$ is zero then all other correlations among $\tilde{\ell}$, $\tilde{\dot{\ell}}$, $\tilde{L}$ and $\tilde{L}'$ are zero.

The results of the previous paragraph assume that the errors in $\tilde{\tau}_{d_1}$ and $\Delta\tilde{\tau}_{d_1}$ are independent of the errors in $\tilde{\tau}_{d_2}$ and $\Delta\tilde{\tau}_{d_2}$. This is clearly so for noise-caused errors; on the other hand, to the extent that the two echoes are coherent, it will not be so for errors caused by variations in the echo power from its mean value. In the next chapter it will be assumed that the two echoes are perfectly coherent – a good approximation when parallel pulses ($\Delta T'' = 0$) are used as in coherent processing. When roof-top pulses ($\Delta T' = 0$) are used, as is typically done for incoherent processing, the two echoes may not be coherent for a turning target, but are likely to be close to perfectly coherent for non-turning targets. If the two echoes are perfectly coherent then a portion of these errors in $\tilde{\tau}_{d_1}$ and $\tilde{\tau}_{d_2}$ and in $\Delta\tilde{\tau}_{d_1}$ and $\Delta\tilde{\tau}_{d_2}$ will be identical and hence will not cause errors in measurement of $\dot{\ell}$ and L', but will cause doubled errors in measurement of ℓ and L'. In this case Eqs. 22 and 25 should be modified by doubling the first term under the final square root when using them to determine σ_ℓ and $\sigma_{L'}$, and eliminating it for $\sigma_{\dot{\ell}}$ and $\sigma_{\dot{L}'}$.

4.4 Selection of signal and signal-processing parameters

Consider signal parameters first. To remove the correlations in Eq. 28, it is reasonable to set $\Delta T' = 0$. Let $f_o = (f_{o_1} + f_{o_2})/2$ and $T = (T_1 + T_2)/2$. For practical reasons $f_{o_1} \approx f_{o_2} \approx f_o$ and $T_1 \approx T_2 \approx T$, approximately if not indeed identically; therefore $B_1 \approx B_2 \approx B$, $|\gamma^M_{FM_1}|^2 \approx |\gamma^M_{FM_2}|^2 \approx |\gamma^M_{FM}|^2$ and $\Delta T'' \approx 2\, f_o\, T/B$. Usually $\Delta T''$ is much greater than ΔT; therefore the choice of ΔT is unimportant. From Eqs. 22 to 27 it is clear with regard to measurement of ℓ and L' that B should be made as large as possible provided that the signal-to-background ratio is not degraded too much and that the spread of $|\gamma^M_{FM}|$ is not made too large. From Eqs. 9b and 10b it follows that making T smaller increases the B that minimizes the spread of $|\gamma^M_{FM}|^2$ at the largest doppler of interest and hence allows a larger B to be used without making the spread of $|\gamma^M_{FM}|^2$ too large. On the other hand, again from Eqs. 22 to 27 it is clear with regard to measurement of $\dot{\ell}$ and L' that B should be made as small as possible provided that the spread of $|\gamma^M_{FM}|$ is not made too large, since this makes $\Delta T''$ larger. Increasing T also makes $\Delta T''$ larger and at the same time, from Eqs. 9b and 10b, allows a smaller B to be used while increasing the spread of $|\gamma^M_{FM}|^2$ the least.

Thus there are conflicting requirements in signal parameters – small T, large B for good ℓ and L' measurement, and large T, small B for good $\dot{\ell}$ and $\dot{L}'$ measurements – that must be traded-off.

The major signal-processing parameters of importance are the threshold on signal-to-noise ratio required to make global errors negligible and $T_s \approx T_{s_1} \approx T_{s_2}$. With regard to local errors it is clear from Eqs. 22 and 23 that the lower T_s is, the better, provided it exceeds the spread of $|\gamma^M_{FM}(\tau,\alpha_o)|^2$. On the other hand, increasing T_s alleviates the global error problem by smoothing the noise, as already mentioned. In fact the optimum choice for T_s to minimize global errors is $\Delta\tau_d$ since, from Eq. 22, further increase in T_s degrades the signal-to-noise ratio. Thus selection of T_s is a tradeoff between global and local errors. Since the smoothed noise power has a chi-squared distribution if the noise is gaussian, it is possible to determine an appropriate signal-to-noise ratio threshold that makes the probability of global errors negligible, as will be seen in the example below.

As an example consider a signal with $f_{o_1} = f_{o_2} = 3{,}500$ Hz and $T_1 = T_2 = \Delta T = 0.5$ s and suppose the maximum $|\alpha_o - 1|$ of interest is 0.02. From Ch. 1, the B that minimizes the spread of $|\gamma^M_{FM}(\tau, 1 \pm 0.02)|^2$ is roughly 217 Hz, with a corresponding spread of 6.8 ms. If $B_1 = B_2 = 217$ Hz and the two FM pulses in the signal have opposite slopes, $\Delta T' = 0$ and $|\Delta T''| = 160$ (which is much larger than ΔT). For $T_s = 20$ ms, $2BT_s \approx 8$; hence the smoothed noise power has a chi-squared distribution with eight degrees of freedom. If the noise level is normalized to 1, for a signal-to-noise ratio of 4 (6 dB) the expected signal-plus-noise level is 5 and the half-signal-power level is 3. A sample of a chi-squared distribution with eight degrees of freedom exceeds three times its mean for 0.229% of the time. If the search for the level crossings is carried out over 500 ms – a reasonable interval for a target of length not exceeding roughly 100 ms whose rough position is known from the detection process – there will be 25 samples and hence a 6% probability of noise exceeding the level. This probability of global error is unacceptably high; however for the slightly higher signal-to-noise ratio of 6 (7.8 dB) this probability of global error drops to 0.25%. Of course if the noise is not gaussian – as is quite likely at the tails we are interested in – these figures will change, but the general form of the result is the same. In any case, a signal-to-noise ratio of 6 would seem to be a good threshold below which measurement should not be attempted.

Figure 5 gives a plot of the standard deviation of $\tilde{\ell}$ as a function of apparent length, assuming incoherent echoes for a signal-to-noise ratio of 6 and $|\alpha_o - 1|$ equal to 0.00 and 0.02 when the signal described above is used. On this figure the ordinary lines represent values computed using Eqs. 22 and 23, while the dashed lines represent interpolations in the region where the spread of $|\gamma^M_{FM}|^2$ approximates the apparent target length (in time) and

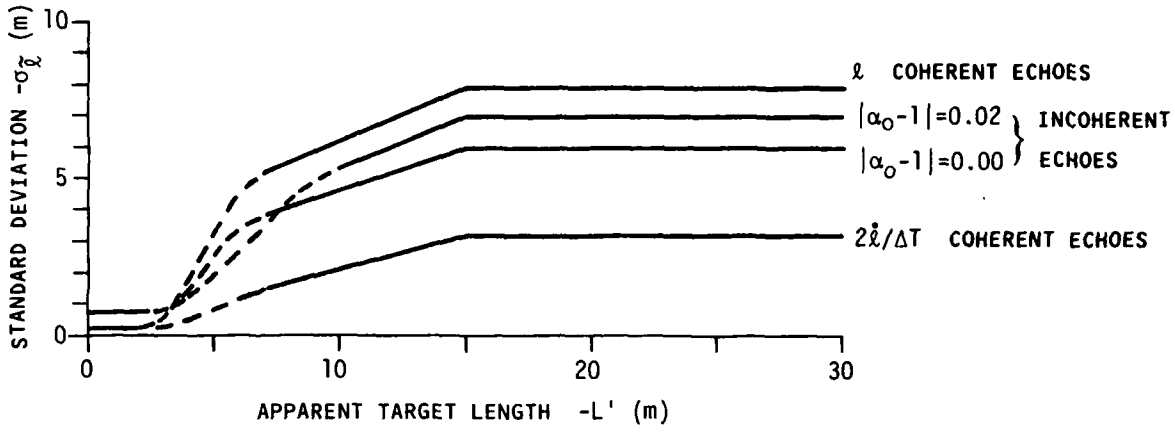

FIG. 5 PATH LENGTH ERROR STANDARD DEVIATION FOR EXAMPLE

hence neither Eqs. 22 or 23 applies. The standard deviation for $\tilde{\dot{\ell}}$ can be found by taking that of $\tilde{\ell}$ and dividing by $\Delta T''/2 = 8$ for m/s or by 4 for knots. The measurements $\tilde{L}'$ and $\tilde{\dot{L}}'$ cannot be made for L' less than 15 m; for L' greater than 15 m their standard deviations are the same as the corresponding standard deviations of $\tilde{\ell}$ and $\tilde{\dot{\ell}}$. Note that the difference in standard deviation between no doppler and maximum doppler is small — probably less than the accuracy of the results. Figure 5 also gives the standard deviations for $\tilde{\ell}$ and $2\tilde{\dot{\ell}}/\Delta T''$ assuming coherent echoes and no-doppler effect and all other conditions the same. As before, for $L' > 15$ m the standard deviations for $\tilde{L}'$ and $\tilde{\dot{L}}'$ are the same as the corresponding error standard deviations of $\tilde{\ell}$ and $\tilde{\dot{\ell}}$.

5 COHERENT MEASUREMENTS

This chapter follows the same general outline as that of the previous. First, the measurement of $\dot{\ell}$ and β is reduced to an estimation of the position of the maximum correlation in time and frequency between the matched filter outputs for the echoes from the two FM pulses. Second, the use of Plaisant's approach *[9,10]* for the estimation of this position is studied. Third, the standard deviations and correlations of the errors in measuring target properties are related to the like properties of estimation errors in the position of the correlation peak. Fourth, consideration is given to the selection of appropriate signal and signal-processing parameters. Finally, incoherent and coherent measurement are compared.

5.1 Basic measurement principle

Consider, first, frequency correlation. From *[2]*,

$$H_i^M(f) \approx F\{L'[(1-\beta\,\Delta t_{T_i}-a)(f+f_{o_i})-\beta(f_{o_i}/k_i)(f+\frac{\dot{\ell}}{2c}f_{o_i})]/(LC)\} \quad \text{(Eq. 29)}$$

(As in the previous chapter, $c^2/(c-\dot{\ell})^2$ has been approximated by unity.) Since the correlation peak in frequency measures the frequency shift between $H_1^M(f)$ and $H_2^M(f)$, the form

$$H_2^M(f) = H_1^M(f-\Delta f^0) \quad \text{(Eq. 30)}$$

is sought. From Eq. 29, Eq. 30 will hold if

$$\left[1-\beta\left(\Delta t_{T_1}+\frac{f_{o_1}}{k_1}\right)-a\right]\Delta f^{o} = \beta(\Delta T+\Delta T")f-(f_{o_2}-f_{o_1}) + \beta\left[(\Delta T+\frac{\dot{\ell}}{2c}\Delta T")\frac{f_{o_2}+f_{o_1}}{2}+\beta\frac{\dot{\ell}}{2c}\left(\frac{f_{o_2}}{k_2}+\frac{f_{o_1}}{k_1}\right)\left(\frac{f_{o_2}-f_{o_1}}{2}\right)\right] \qquad \text{(Eq. 31)}$$

Because H_1^M and H_2^M are being observed through the windows $\Gamma_{FM_1}^M$ and $\Gamma_{FM_2}^M$, which are low-pass filters with bandwidths B_1 and B_2, $f_{o_2}-f_{o_1}$ must be small compared with B_1 and B_2; therefore there is no reason not to select $f_{o_2} = f_{o_1} = f_o$. In addition, Δf should not depend upon f because otherwise there will be a stretch as well as a shift between H_1^M and H_2^M; therefore $\Delta T+\Delta T"$ should be close to zero or, since $\Delta T"$ is much larger than ΔT, $\Delta T"\approx 0$. Again there is no reason not to select $k_2 = k_1 = k$ and $T_1 = T_2 = T$, in which case $\Gamma_{FM_1}^M = \Gamma_{FM_2}^M = \Gamma_{FM}^M$, $B_2 = B_1 = B$ and $\Delta T" = 0$. Finally a and $\beta\Delta t_{T_1}$ are negligible with respect to 1, but $\beta f_o/k$ is not. With all these factors Eq. 31 becomes

$$\Delta f^{o} = \beta\,\Delta T\, f_o/(1-\beta f_o/k)\ . \qquad \text{(Eq. 32)}$$

To measure Δf^o we would like to correlate H_1^M and H_2^M, but we have available only ϕ_1^D and ϕ_2^D. From Eqs. 6 and 7, if segments of ϕ_1^M and ϕ_2^M of length T_F centred on τ_o are Fourier transformed, H_1^M and H_2^M can be observed through the window provided by Γ_{FM}^M. For the moment, assume that T_F is sufficiently long to include the entire echo. The first matched-filter output ϕ_1^D must be advanced by $\Delta\tau^o$ to align the echo contained in it with the echo contained in ϕ_2^D. Further assume for the moment that the noises $n_1(\tau)$ and $n_2(\tau)$ are zero and let $\Phi_1'(f)$ be the fourier transform of $\phi_1^D(\tau+\tau^o-\Delta\tau^o,1)$ and $\Phi_2(f)$ be the fourier transform of $\phi_2^D(\tau+\tau^o,1)$. From Eqs. 6 and 7

$$\Phi_1'(f) = e^{-2\pi j\left[f_o'(\tau_{d_1}'-\tau_{d_1}) + f(\tau_{d_1}-\tau^o+\Delta\tau^o)\right]}\Gamma_{FM}^M(f-f_o')\, H_1^M(f-f_o') \quad ,$$

$$\Phi_2(f) = e^{-2\pi j\left[f_o'(\tau_{d_2}'-\tau_{d_2}) + f(\tau_{d_2}-\tau^o)\right]}\Gamma_{FM}^M(f-f_o')\, H_2^M(f-f_o') \quad ,$$

(Eq. 33)

where from Eq. 26 of *[2]*

$$\tau_{d_1}'-\tau_{d_1} = \tau_{d_2}'-\tau_{d_2} = -\,[\dot{\ell}/(c-\dot{\ell})](f_o/k) \quad .$$

It follows from Eqs. 30 and 33 that to align $\Phi_1^{M'}$ and $\Phi_2^{M'}$ in frequency, Φ_1^M must be advanced by Δf^o , but from Eq. 17 of *[2]* and Eq. 8

$$\Gamma[f\ ;\ (B-|\alpha_o-1|f_o)/2]\ \Gamma_{FM}^M(f-\Delta f;\ \alpha_o) = e^{-2\pi j(\alpha_o-1)(2f\Delta f-\Delta f^2)/k} \cdot \Gamma[f-\Delta f;\ (B-|\alpha_o-1|f_o)/2]\Gamma_{FM}^M(f) \ ;$$

(Eq. 34)

therefore,

$$\Gamma[f-f_o'-\Delta f^o;\ (B-|\alpha_o-1|f_o)/2]\ \Phi_2(f)$$

$$= e^{-2\pi j\{f[(\dot{\ell}/c)(\Delta T+2\Delta f^o/k)-\Delta\tau^o]+\ \Delta f^o[\ell/c-(\dot{\ell}/c)\frac{\Delta T}{2}+\frac{2f_o'+\Delta f^o-f_o}{k}-\tau^o+\Delta\tau^o]\}}$$

$$\Gamma[f-f_o';\ (B-|\alpha_o-1|f_o)/2]\ \Phi_1'(f-\Delta f^o)$$

$$\approx e^{-2\pi j\Delta f^o\{[\ell+\dot{\ell}(\Delta T/2-f_o/k)]/c-\tau^o\}}$$

$$\Gamma[f-f_o;\ (B-|\alpha_o-1|f_o)/2]\Phi_1'(f-\Delta f^o) \qquad \text{(Eq. 35)}$$

if

$$\Delta\tau^o = (\dot{\ell}/c)(\Delta T + 2\Delta f^o/k) \quad . \qquad \text{(Eq. 36)}$$

Thus if $\phi_1^D(\tau,l)$ is advanced in time by $\Delta\tau^o$ and in frequency by Δf^o, it will be identical to $\phi_2^D(\tau,l)$ over the frequency band in common between the two, except for a phase shift. This phase shift may be removed from correlation in time and frequency between ϕ_1^D and ϕ_2^D by taking the magnitude of the correlation. The next section discusses one method of estimating the position of the correlation peak and hence $\Delta\tau^o$ and Δf^o. Given such estimates of $\widetilde{\Delta\tau}^o$ and $\widetilde{\Delta f}^o$, β and $\dot{\ell}$ may be estimated using Eqs. 32 and 36:

$$\widetilde{\beta} = \frac{\widetilde{\Delta f}^o}{f_o \Delta T} \Big/ \left(1 + \frac{\widetilde{\Delta f}^o}{k\Delta T}\right) ,$$

$$\widetilde{\dot{\ell}} = \frac{c\,\widetilde{\Delta\tau}^o}{\Delta T} \Big/ \left(1+2\,\frac{\widetilde{\Delta f}^o}{k\Delta T}\right) . \qquad \text{(Eq. 37)}$$

In general, of course, $\widetilde{\Delta\tau}^o$ and $\widetilde{\Delta f}^o$ will contain errors and therefore the phase shift $\Delta\phi^o$ at $\widetilde{\Delta\tau}^o$, $\widetilde{\Delta f}_o$ will differ greatly from that given in Eq. 35. In fact, from Eq. 35

$$\Delta\phi^o \approx 2\pi \left(f_o(\Delta\tau^o - \widetilde{\Delta\tau}^o) + \widetilde{\Delta f}^o\{[\ell+\dot{\ell}(\Delta T/2 - f_o/k)]/c - \tau^o\} \right) \qquad \text{(Eq. 38)}$$

Clearly if $|\Delta\tau^o - \Delta\tau^o| < 1/2\, f_o$ so that there are no problems with the ambiguity in measuring phase, Eqs. 36 and 38 can be used to obtain an improved estimate $\dot{\ell}'$ of $\dot{\ell}$ from an estimate $\Delta\phi^o$ of $\Delta\phi^o$:

$$\widetilde{\dot{\ell}}' = \frac{c}{f_o \Delta T} \left[\frac{\widetilde{\Delta\phi}^o}{2\pi} + f_o \widetilde{\Delta\tau}^o - \widetilde{\Delta f}_o(\widetilde{\ell}/c - \tau^o) \right] \Big/ \left(1 + \frac{\widetilde{\Delta f}^o}{k\Delta T}\right) . \qquad \text{(Eq. 39)}$$

In general, the segments of ϕ_1^D and ϕ_2^D when fourier transformed will be approximately centred on the echoes and hence $\tau^o \approx \widetilde{\ell}/c$.

If $\phi_1^D(\tau,l)$ is advanced in time by $\Delta\tau^o$, in frequency by Δf^o, and rotated by $\Delta\phi^o$, then added to $\phi_2^D(\tau,l)$ and the centre τ_d and spread $\Delta\tau_d$ of the echo contained in the result estimated (by using, for example, the technique of Section 3.2), ℓ and L' may be estimated using Eqs. 16 and 18:

$$\widetilde{\ell} = c\,\widetilde{\tau}_d - \widetilde{\dot{\ell}}(\Delta T + \Delta T')/2 ,$$

$$\widetilde{L}' = c\,\widetilde{\Delta\tau}_d \Big/ \left[2 - \widetilde{\dot{\beta}}(\Delta T + \Delta T')\right] . \qquad \text{(Eq. 40)}$$

5.2 Plaisant's approach to estimation of the correlation peak

Consider finding the correlation peak in time and frequency between ϕ_1^D and ϕ_2^D as follows: select a time advance $\Delta\tau$, fourier transform segments of length T_F containing the echo with the segment for ϕ_1^D advanced by $\Delta\tau$ with respect to that for ϕ_2^D. Cross-correlate the results, Φ_1' and Φ_2, in frequency and find the position of the peak by averaging the two frequencies at which the magnitude of the cross correlation falls to one half of its maximum value. Repeat this process for a series of $\Delta\tau$ retaining the position in fequency and the magnitude of the peak for each τ. Finally find the position of the peak in time by averaging the two times at which the series of frequency peaks fall to one half its maximum. Of course it would have been just as valid to shift ϕ_1^D by a series of frequency shifts and cross-correlate each in time with ϕ_2^D. In either case it is clear that the process of estimating $\Delta\tau^o$ and Δf^o is not independent; nevertheless it will be assumed the correlation between errors in these two estimates may be neglected.

Now consider the error in estimation of one of the half-peak correlation points in frequency. As before, the standard deviation σ_f' of this error is obtained by dividing the standard deviation of the magnitude of correlation at such a point by the slope of this expected value. Near the correlation peak the correlation in frequency between the two matched-filter outputs when noise is absent is, except for a rotation, the auto-correlation of a segment $B-(|\alpha_o-1| -|\beta|\Delta T)f_o$ wide in frequency of the transfer function. In Appendix D it is shown that the one-half correlation points are $0.6/T^*$ distant from the peak and hence will be close to the peak if $B-(|\alpha_o-1|-|\beta|\Delta T)f_o T^*$ is large compared with one. In this case the magnitudes of the correlation at the one-half correlation points are approximately equal and only the variation about these values caused by the addition of noise is of interest. Computation of the mean and variance of the magnitude of correlation is facilitated by the fact that when the standard deviation of a complex random variable is small compared with its mean, the mean of the magnitude of the random variable is very close to the magnitude of the mean of that variable and the variance of the magnitude of the random variable is one-half that of the variance of the random variable itself (since it can vary in two directions, but only variation in the direction of the mean counts in the magnitude).

The mean and variance of the correlation in frequency between the two matched filter outputs is readily obtained, since the noise in each matched-filter output is a segment of band-passed white noise and the echo may be approximated as such if the spread of $|\gamma_{FM}^M|^2$ is small compared with the apparent target length. Details are given in Appendix D; the result is

$$\sigma_f' = \frac{B-|\alpha_o-1|f_o}{2[B-(|\alpha_o-1|+|\beta|\Delta T)f_o]T^*}\sqrt{\frac{1}{B\ T_F}\left[\frac{2}{S/N}+\frac{1}{(S/N)^2}\right]} \qquad \text{(Eq. 41)}$$

where

$$T^* = \min [\Delta\tau_d , T_F]$$

$$S/N = \sigma_e^2(B-|\alpha_o-1|f_o)T^* /(\sigma_n^2 B^2 \Delta\tau_d T_F)$$

(Note that S/N is the signal-to-noise ratio in output power of the matched filters after smoothing over an interval of T_F) Unlike in the previous chapter it is not obvious that errors in the measurements of the two half-peak-correlation frequencies are uncorrelated; in fact it is shown that there is a correlation between the variation in the correlation function at these two points but that, to the accuracy of this development, it can be neglected.

The problem of finding the errors in the half-peak-correlation points in time is exactly analogous except that time replaces frequency and vice versa. The result is

$$\sigma'_\tau = \frac{B-|\alpha_o-1|\ f_o}{2[B-(|\alpha_o-1|+|\beta|\Delta T)f_o]^2} \sqrt{\frac{1}{B\ T_F}\left[\frac{2}{S/N} + \frac{1}{(S/N)^2}\right]} \qquad \text{(Eq. 42)}$$

Given expressions for the standard deviations in estimation of the half-peak-correlation frequencies and times, σ'_f and σ'_τ , the standard deviations $\sigma_{\Delta f}$ and $\sigma_{\Delta\tau}$ of the estimates $\widetilde{\Delta f}^o$ and $\widetilde{\Delta\tau}^o$ are

$$\sigma_{\Delta f} = \sigma'_f/\sqrt{2} , \qquad \sigma_{\Delta\tau} = \sigma'_\tau/\sqrt{2} . \qquad \text{(Eq. 43)}$$

The errors in the estimates $\widetilde{\Delta f}^o$ and $\widetilde{\Delta\tau}^o$ are, by assumption, uncorrelated. In addition, the phase $\Delta\phi^o$ of the double correlation at $\widetilde{\Delta\tau}^o$, $\widetilde{\Delta f}^o$ can be estimated by taking the arctangent of the ratio of the real and imaginary parts of the double correlation function evaluated at $\widetilde{\Delta\tau}^o$, $\widetilde{\Delta f}^o$. The error in this phase measurement is shown in Appendix D to have a standard deviation of

$$\sigma_{\Delta\phi} = \frac{B-|\alpha_o-1|f_o}{B-(|\alpha_o-1|+|\beta|\Delta T)f_o} \sqrt{\frac{1}{2B\ T_F}\left[\frac{2}{S/N} + \frac{1}{(S/N)^2}\right]} . \qquad \text{(Eq. 44)}$$

5.3 Measurement error means and standard deviation

Given any technique for estimating $\Delta\tau^o$, Δf^o and $\Delta\phi^o$ — such as Plaisant's approach, just covered — then the standard deviations σ_β, $\sigma_{\dot{\ell}}$ and $\sigma'_{\dot{\ell}}$ of the error in the estimates $\tilde{\beta}$, $\tilde{\dot{\ell}}$ and $\tilde{\dot{\ell}}'$ are readily obtainable from $\sigma_{\Delta\tau}$, $\sigma_{\Delta f}$ and $\sigma_{\Delta\phi}$ by use of Eqs. 37 and 39. The last multiplicative factors in the equations are for $\tilde{\beta}$, $\tilde{\dot{\ell}}$ and $\tilde{\dot{\ell}}'$, given there are corrections close to unity; therefore errors in these factors may be neglected; hence

$$\sigma_\beta = \sigma_{\Delta f}/(f_o\,\Delta T), \qquad \sigma_{\dot{\ell}} = \sigma_{\Delta\tau}\, c/\Delta T\ ; \qquad \sigma'_{\dot{\ell}} = \sigma_{\Delta\phi}\, c/2\pi\, f_o\,\Delta T \qquad \text{(Eq. 45)}$$

An important point to note is the inverse dependence of these standard deviations on ΔT, the time difference between the two pulses of the signal.

Given any technique for measuring the delay and spread of the combined echoes — such as Plaisant's approach, covered in Sect. 3.2 — then the second-order statistical properties of the estimates $\tilde{\ell}$ and $\tilde{L}'$ are readily obtainable from σ_{τ_d} and $\sigma_{\Delta\tau_d}$ by use of Eq. 40. Note that if Plaisant's approach is used, the signal-to-noise ratios in Eqs. 22 to 25 should be doubled, because of the coherent adding of the two echoes. It would appear from Eq. 40 that $\tilde{\ell}$ contains an error that depends on the error in $\tilde{\dot{\ell}}$, and similarly that $\tilde{L}'$ contains an error that depends on the error in $\tilde{\beta}$. However, the error in $\tilde{\dot{\ell}}$ also causes an error in adding the two echoes; this cancels the apparent error in Eq. 40, and similarly for $\tilde{L}'$ and $\tilde{\beta}$. The error in aligning the echoes in time will however cause an error in $\tilde{L}'$; hence

$$\sigma_\ell = c\ \sigma_{\tau_d}\ ,$$

$$\sigma_{L'} = \sqrt{(c\,\sigma_{\Delta\tau_d})^2+(\Delta T\,\sigma_{\dot{\ell}})^2}\ /2 = c\ \sqrt{(\sigma_{\Delta\tau_d})^2}\ /2\ ,$$

$$\rho_{\dot{\ell}L'} = \Delta T\ \ \sigma_{\dot{\ell}}/(2\sigma_{L'}) = \sigma_{\Delta\tau}/\sqrt{(\sigma_{\Delta\tau_d})^2 + (\sigma_{\Delta\tau})^2}\ . \qquad \text{(Eq. 46)}$$

5.4 Selection of signal and signal-processing parameters

The two key signal parameters determining performance of coherent measurement algorithms are ΔT and B. Obviously from Eq. 45 the spread between the two FM pulses should be made as large as possible as long as coherence between the two echoes is maintained. Furthermore, from Eqs. 41 to 44 it is

clear that B should be made as large as possible provided that the signal-to-noise ratio is not degraded too much and that the spread of $|\gamma^M_{FM}|^2$ is not made too large. As has already been pointed out in Sect. 3.4, from Eq. 9b, use of a smaller T increases the value of B that may be used without making the spread of $|\gamma^M_{FM}|^2$ too large. With regard to the incoherent processing used in conjunction with the coherent processing to measure ℓ and L', it is clear from Eq. 46 and the discussion of Sect. 3.4 that performance is maximized under the same conditions. Thus for coherent measurements there are no conflicts in choice of signal parameters — small T and large B are desirable for ℓ, $\dot{\ell}$, L' and β.

The major signal-processing parameters of importance are T_F and the threshold on signal-to-noise ratio required to make global errors negligible. With regard to local errors it is clear from Eqs. 41, 42, and 44 that T_F should be set equal to $\Delta\tau_{d_F}$ to minimize the probability of global errors, again because that maximizes the signal-to-noise ratio. Selection of a suitable threshold on signal-to-noise ratio required to make global errors negligible is not a straightforward analytical problem and is best solved by use of simulation and sea trials.

As an example, consider a signal with $f_o = 3.500$ Hz, $T = 0.5$ and $\Delta T = 1$ s and suppose the maximum $|\alpha_o - 1|$ of interest is 0.02. As already noted, the B that minimizes the spread of $|\gamma^M_{FM}|^2$ for $|\alpha_o - 1| = 0.2$ is 217 Hz, with a corresponding spread of 6.8 ms. For this signal $|\Delta T'| = 160$. Take $T_F = 50$ ms as a reasonable average value of $\Delta\tau_d$. Figure 6a is a plot of the standard deviation of $\tilde{\beta}$ versus apparent length for a signal-to-noise ratio of 6 and the signal just described for $|\alpha_o - 1| = 0.0$ and 0.02 and $\beta = 0.0$ and 20 mrad/s (a turning rate $\dot{\alpha}$ of 20 mrad/s corresponds to a complete turn in 5 minutes). For comparison with Fig. 5, note that measuring β by $\tilde{L}'/\tilde{L}'$ gives an error standard deviation of

$$\sigma_\beta \approx \frac{1}{L'} \sqrt{\sigma^2_{\dot{L}'} + \sigma^2_{L'} \beta} \approx \sigma_{\dot{L}'}/L' \quad ,$$

which for the case under consideration, coherent echoes, and a target of 40 m, is 10 mrad/sec. Figure 6b is a plot of the standard deviation of $\tilde{\dot{\ell}}$ versus apparent length for the same conditions as in Fig. 6a. For comparison with Fig. 5 note that it gives a $\sigma_{\dot{\ell}}$ of 0.8 kn for coherent echoes and a target of 40 m.

To use the phase at $\tilde{\Delta\tau}^o$, $\tilde{\Delta f}^o$ to improve the estimate of $\dot{\ell}$ requires that $|\tilde{\Delta\tau}^o - \Delta\tau^o|$ be less than $1/2\ f_o$ or that the error in $\tilde{\ell}$ be less than

$c/2f_o\Delta T$, which for the example is 0.43 kn, to prevent ambiguities in phase. It is clear from Fig. 6b that this will not in general be the case for the example. If it were not for problems with ambiguity in phase, in the example the standard deviation of the error in $\tilde{\dot{\ell}}'$ would be, from Eqs. 44 and 45, 0.02 kn for $\alpha_o - 1 = \beta = 0$; therefore it is indeed unfortunate that use may not be made of phase to improve the measurement of $\tilde{\dot{\ell}}$.

5.5 Comparison of coherent and incoherent measurements

Although the examples given in Sects. 4.4 and 5.4 by no means consider optimized signal and signal-processing parameter values, the parameter values used are not untypical of what might be used in practice. Therefore it is possible to derive some general conclusions based on these examples and on the analysis that preceeded them. In the first place, incoherent processing does relatively better in measuring $\dot{\ell}$, while coherent processing does relatively better in measuring β . In the second place, even though ℓ and L' are measured incoherently with coherent processing, there is a roughly 3 dB gain in signal-to-noise ratio made possible by the coherent addition of the echoes from the two pulses prior to this incoherent processing. One advantage with the coherent processing is that there is no conflict in choice of signal parameters for best measurement of $\dot{\ell}$ and β as opposed to ℓ and L' . On the other hand, coherent processing breaks down if the apparent target length is too short.

The major reason that incoherent processing does better than coherent processing in measuring $\dot{\ell}$ is the fact that $\Delta T''$ is not zero for incoherent processing. A signal with non-zero $\Delta T''$ can be used in coherent processing at the cost of increased processing complexity. If such a signal is used, it is necessary to correlate the second echo with versions of the first echo that are shifted in time and are both shifted in frequency and stretched in frequency, where the stretch in frequency is necessary to compensate for the stretch in frequency of the envelope of the second echo caused by non-zero $\Delta T''$. The advantage of such a signal is that it can be processed incoherently if L' is too small. The disadvantage of such a signal, in addition to the increased processing complexity, is the presence of a conflict in choice of signal parameters between those that are best for $\dot{\ell}$ and those that are best for the remaining measurements.

6 SPACE/FREQUENCY MEASUREMENTS

This chapter follows the same general outline as that of the previous one. First, measurement of target bearing and apparent aspect is reduced to estimation of the position of the peak in correlation in time and frequency between the matched-filter outputs for the echoes from two hydrophones (or two separated arrays of hydrophones). Second, use of Plaisant's approach *[9,10]* to the estimation of the position of the correlation peak is studied.

Third, target aspect and standard deviations and correlations of the errors in bearing measurement are related to the like properties of estimation errors in the position of the correlation peak. Fourth, consideration is given to selection of appropriate signal and signal-processing parameters.

6.1 Basic measurement principle

Consider the geometry given in Fig. 7 and how the matched-filter output for an FM pulse depends on the bearing ψ with respect to the array, the aspect α, and the hydrophone displacement Δx_H from an arbitrary reference point along the receiver reference line. If the range r_R of the target from the receiver reference point is large, the change $\Delta\alpha$ in aspect caused by Δx_H is

$$\Delta\alpha = \Delta x_H \sin\psi / r_R \quad . \qquad \text{(Eq. 47)}$$

Now let $H_i^M(f,\Delta x_H)$ be the $H_i^M(f)$ corresponding to a hydrophone at Δx_H. The only variable in Eq. 29 significantly changed by the change in aspect from α to $\alpha + \Delta\alpha$ is L'; therefore to find $H_i^M(t,\Delta x_H)$, L' must be replaced by $(L'+\Delta\alpha \frac{\partial L'}{\partial\alpha})$. Furthermore, it is obvious from Eq. 26 of *[6]* and from Eq. 16 that $\tau'_{d_i} - \tau_{d_i}$ is unchanged but that, in τ_d, ℓ must be replaced by $\ell+\Delta\ell$ where, from Fig. 7,

$$\Delta\ell = \Delta x \cos\psi \qquad \text{(Eq. 48)}$$

Now suppose that there are two hydrophones located at $\pm \Delta x_H$. It is clear that differences in L' and ℓ — whether caused by the use of two hydrophones separated in space or by two identical pulses separated in time — have exactly the same effect; therefore from Sect. 4.1 it is clear that if the matched-filter output for a single pulse for the hydrophone at $-\Delta x_H$ is correlated with that for the hydrophone at Δx_H, the correlation peak will, in analogy with Eqs. 32 and 38, have a correlation peak at

$$\Delta f_i^o = \beta_x \Delta x f_{o_i} /(1-\beta f_{o_i}/k_i) ,$$

$$\Delta\tau_i^o = (\Delta x \cos\psi + 2 \dot{\ell} \Delta f_i^o/k_i)/c, \qquad \text{(Eq. 49)}$$

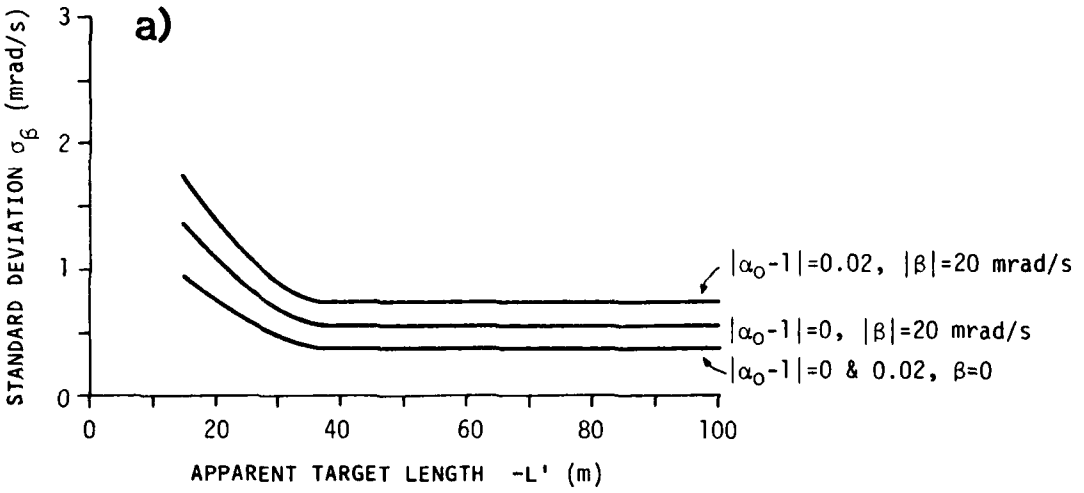

FIG. 6a APPARENT TURNING RATE ERROR STANDARD DEVIATION FOR EXAMPLE

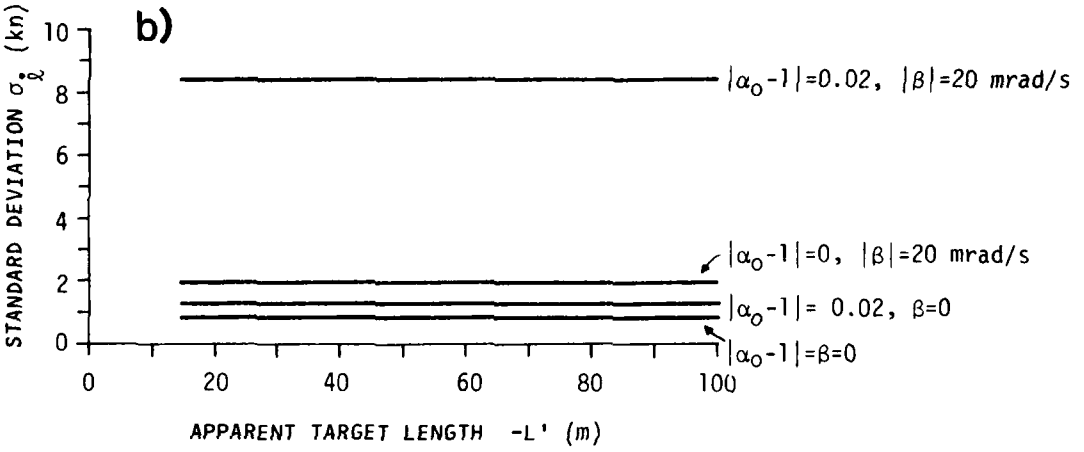

FIG. 6b PATH LENGTH RATE ERROR STANDARD DEVIATION FOR EXAMPLE

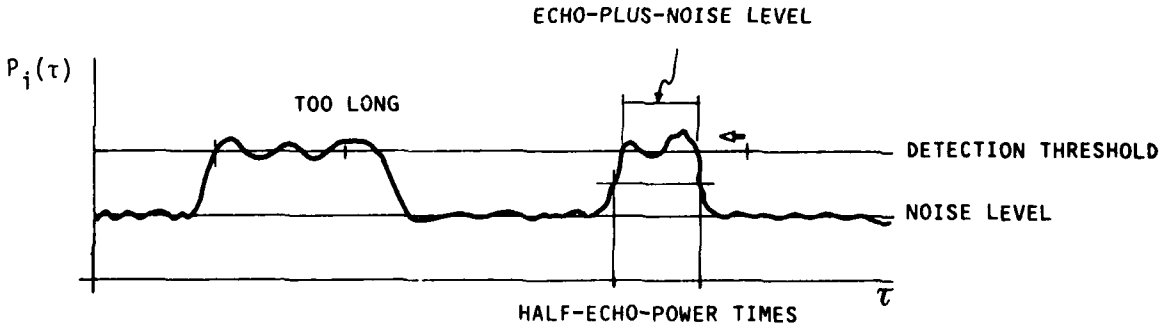

FIG. 7 ESTIMATING ECHO-PLUS-NOISE POWER LEVEL AND FINDING THE HALF-ECHO-POWER TIMES

where $\Delta x \triangleq 2\Delta x_H$ is the separation between the two hydrophones and — in analogy with β —

$$\beta_x = -\frac{1}{L'}\left(\frac{\partial \dot{L}'}{\partial \alpha}\frac{\Delta\alpha}{\Delta x} + \frac{\partial L'}{\partial \gamma}\frac{\Delta\gamma}{\Delta x}\right)$$

$$= \frac{2\sin\alpha}{\cos\alpha + \cos(\alpha-\gamma)}\,\frac{\sin\psi}{r_R} \qquad \text{(Eq. 50)}$$

from Eqs. 18 and 47. (Note that from Eq. 3 that $\beta = -\frac{1}{L'}\left(\frac{\partial L'}{\partial \alpha}\frac{\Delta\alpha}{\Delta T} + \frac{\partial L'}{\partial \gamma}\frac{\Delta\gamma}{\Delta T}\right)$ and that the change in γ caused by Δx is the same as that caused in α.)

These relationships may be used in two measurement schemes based respectively on incoherent and coherent time-processing of the matched-filter outputs for each hydrophone from the two FM pulses. In the incoherent approach, the two matched-filter outputs from the two hydrophones for the echoes from each pulse are correlated in time and frequency to obtain the estimates $\widetilde{\Delta\tau}_i^o$ and $\widetilde{\Delta f}_i^o$ for $i = 1, 2$ and then the phases $\widetilde{\Delta\phi}_i$ at these points estimated. Next, for each pulse the two matched-filtered echoes from the two hydrophones are added coherently by time, frequency, and phase shifting of the matched-filtered echoes from the first hydrophone by $\widetilde{\Delta\tau}_i^o$, $\widetilde{\Delta f}_i^o$ and $\widetilde{\Delta\phi}_i^o$. Now the methods of Ch. 3 can be applied to obtain estimates of $\ell, \dot{\ell}, L'$, and $\dot{L}'$ and the estimates $\widetilde{\cos\psi}$ and $\widetilde{\beta}_x$ obtained by averaging the two estimates of each obtained from

$$\widetilde{\cos\psi}_i = (c\,\widetilde{\Delta\tau}_i - 2\,\widetilde{\dot{\ell}}\,\widetilde{\Delta f}_i^o/k_i)/\Delta x\ ,$$

$$\widetilde{\beta}_{x_i} = \widetilde{\Delta f}_{o_i}(1-\widetilde{\beta}\,f_{o_i}/k_i)/(f_{o_i}\,\Delta x) \qquad \text{(Eq. 51)}$$

with $\widetilde{\beta} = \widetilde{\dot{L}}'/\widetilde{L}'$, which follow from Eq. 48. Alternatively β and β_x may be estimated, following Wiekhorst *[11]* , from

$$\widetilde{\beta} = \left[(\Delta f_2^o/f_{o_2}) - (\Delta f_i^o/f_{o_i})\right] \Big/ \left[(\Delta f_2^o/k_2) - (\Delta f_1^o/k_1)\right]\ ,$$

$$\widetilde{\beta}_x = \Delta f_1^o\,\Delta f_2^o\left[(1/f_{o_1}k_2) - (1/f_{o_2}k_1)\right] \Big/ \left\{\left[(\Delta f_2^o/k_2) - (\Delta f_1^o/k_1)\right]\Delta x\right\}\ , \qquad \text{(Eq. 52)}$$

which also follow from Eq. 48. In any case, if γ and r_R can be

estimated via other means α may be estimated from Eq. 49, $\widetilde{\cos}\,\psi$, and $\widetilde{\beta}_x$. For example, in the monostatic case $\beta_x = \frac{2}{\ell} \tan\alpha \sin\psi$ and $\beta = \dot{\alpha} \tan\alpha$; hence $\dot{\alpha}$ and $\tan\alpha$ are readily estimated from Eq. 44, $\widetilde{\cos}\,\psi$, and $\widetilde{\ell}$.

In the coherent approach a parallel double-FM pulse is transmitted and temporal and spatial time and frequency shifts are estimated as follows. The estimates $\widetilde{\Delta\tau}_t^o$ and $\widetilde{\Delta f}_t^o$ of the temporal shifts are found by performing, for each hydrophone, correlations in time and frequency between the two matched-filtered echoes from the two pulses, averaging the two correlation functions, and determining the position of the peak and its phase. In a similar manner, the estimates $\widetilde{\Delta\tau}_x^o$ and $\widetilde{\Delta f}_x^o$ of the spatial shifts are found by performing, for each pulse, correlations in time and frequency between the two matched-filtered echoes from the two hydrophones, averaging the two correlation functions, and determining the position of the peak and its phase. The estimates $\widetilde{\Delta\tau}_t^o$ and $\widetilde{\Delta f}_t^o$ are used to estimate $\cos\psi$ and β_x via

$$\widetilde{\cos}\,\psi = (c\,\widetilde{\Delta\tau}_x^o - 2\,\widetilde{\dot{\ell}}\,\widetilde{\Delta f}_x^o/k)/\Delta x,$$

$$\widetilde{\beta}_x = \widetilde{\Delta f}_x^o(1-\widetilde{\beta}\,f_o/k)/f_o\,\Delta x\,, \qquad \text{(Eq. 53)}$$

which follows from Eq. 48. Finally, by shifting the four matched-filtered echoes — two from each hydrophone — appropriately in time, frequency, and phase, they may be added coherently, the centre τ_d and spread $\Delta\tau_d$ of the combined echo estimated, and Eq. 40 used to determine $\widetilde{\ell}$ and $\widetilde{L}'$.

In analogy with temporal processing, the estimate of $\cos\psi$ obtained via Eqs. 51 or 53 may be improved by use of phase information under appropriate circumstances. The procedure will be described only for the situation in which Eq. 51 is being used as its application; when Eq. 53 is being used the procedure differs only trivially. For the improvement to be possible $|\widetilde{\Delta\tau}_x^o - \Delta\tau_x^o| < 1/2\,f_o$ is required to prevent phase ambiguities. In analogy with Eq. 39, the phase shift $\Delta\phi_x^o$ in the double correlation at $\widetilde{\Delta\tau}_x^o$, $\widetilde{\Delta f}_x^o$ is

$$\Delta\phi_x^o = 2\pi\left\{f_o(\Delta\tau_x^o - \widetilde{\Delta\tau}_x^o) + \widetilde{\Delta f}_x^o\left[(\ell + \Delta x\cos\psi/2 - \dot{\ell}\,f_o/k)/c - \tau^o\right]\right\}. \qquad \text{(Eq. 54)}$$

Finally, in analogy with Eqs. 39, 44 and 53 may be used to obtain the improved estimate

$$\widetilde{\cos}\,\psi' = \frac{c}{f_o\,\Delta x}\left\{\frac{\widetilde{\Delta\phi}^o{}_x}{2\pi} + f_o\,\widetilde{\Delta\tau}^o{}_x - \widetilde{\Delta f}_x^o\left[(\widetilde{\ell} + \widetilde{\dot{\ell}}\,f_o/k)/c - \tau^o\right]\right\}. \qquad \text{(Eq. 55)}$$

The discussion so far has assumed that only two hydrophones are used. In fact in actual practice it is unlikely that only two hydrophones would be used, since the signal-to-noise ratio at a single hydrophone would be small. Instead, an array of hydrophones would be used. A general discussion of space/frequency technique with arrays is beyond the scope of this document; however, an obvious way to use an array is to split it into two subarrays, to use ordinary beamforming for each subarray, and to treat the beamformed outputs as though they were single hydrophone outputs. Obviously performance can be improved if the two subarrays are separated in space, as for example in a towed array consisting of two active sections separated by an inert section.

In this regard it is worth noting that the above procedure can be applied in the time domain: namely a pulse train of pulses is used, which is divided into two sub-pings, each of which is processed by a beamformer that forms beams in doppler rather than in bearing. This approach suffers one defect not present in the spatial analogue, namely range ambiguity – which, however, can be removed by using any of a number of methods discussed by Rihaczek *[12]*. Alternatively, two identical sub-pings may be used, each of which consists of a series of pulses with different centre frequencies. In this case there is no range ambiguity, but for detection the echoes in each sub-ping can be added only incoherently rather than coherently as is the case of pulses with identical centre frequencies. For measurement of $\dot{\ell}$ and β, correlation in time and frequency are performed for both frequencies and then averaged. The net effect is to divided the standard deviation of the measurement error by the square root of the number of pulses per sub-ping. From Eqs. 41 and 42 it follows that this improvement is almost as good as dividing the signal-to-noise ratio by the number of pulses per sub-ping, as would be the case for identical centre frequencies. Furthermore, reverberation problems would not be as great as when the sub-ping consists of identical pulses.

6.2 Plaisant's approach to estimation of the correlation peak

Since the procedure is the same whether the time and frequency shifts have temporal or spatial causes, the discussion of Sect. 4.2 need not be repeated. It is only necessary to modify Eqs. 41 and 42 to reflect the fact that $\cos\psi$ and β_x are being measured rather than $\dot{\ell}$ and β and that correlations for two pulses exist:

$$\sigma'_{f_i} = \frac{B_i - |\alpha_o - 1| f_{o_i}}{2\left[B_i - (|\alpha_o - 1| + |\beta_x| \Delta x) f_{o_i}\right] T^*} \sqrt{\frac{1}{B_i T_F}\left[\frac{2}{S/N_i} + \frac{1}{(S/N_i)^2}\right]},$$

$$\sigma'_{\tau_i} = \frac{B_i - |\alpha_o - 1| f_{o_i}}{2\left[B_i - (|\alpha_o - 1 + 1 \beta_x| \Delta x) f_{o_i}\right]^2} \sqrt{\frac{1}{B_i T_F}\left[\frac{2}{S/N_i} + \frac{1}{(S/N_i)^2}\right]} \qquad \text{(Eq. 56)}$$

for $i = 1, 2$, where T^* is defined as before and

$$S/N_i = \sigma_{e_i}^2 \left(B_i - |\alpha_o - 1| f_{o_i} \right) T^* / (\sigma_n^2 B_i^2 \Delta\tau_d T_f) .$$

Finally Eqs. 43 and 44 become

$$\sigma_{\Delta f_i} = \sigma'_{f_i} / \sqrt{2} \quad , \quad \sigma_{\Delta\tau_i} = \sigma'_{\tau_i} / \sqrt{2} \quad , \qquad \text{(Eq. 57)}$$

$$\sigma_{\Delta\phi_i} = \frac{B_i - |\alpha_o - 1| f_{o_i}}{B_i - (|\alpha_o - 1| + |\beta_x| \Delta x) f_{o_i}} \sqrt{\frac{1}{2B_i T_F} \left[\frac{2}{S/N_i} + \frac{1}{(S/N)^2} \right]}$$

for $i = 1, 2$. For coherent temporal processing, the subscripts should be replaced by x in these equations and the signal-to-noise ratio doubled.

6.3 Means and standard deviation of the measurement error

If incoherent temporal processing is used with Eq. 51 to estimate $\cos\psi$ and β_x, the errors in the correction terms due to $\tilde{\ell}$ and $\tilde{\beta}$ may be neglected, was done as before, to yield

$$\sigma_{\beta_{x_i}} = \sigma_{\Delta f_i} / (f_{o_i} \Delta x) \quad , \quad \sigma_{\cos\psi_i} = \sigma_{\Delta\tau_i} c / \Delta x \quad , \quad \sigma'_{\cos\psi_i} = \sigma_{\Delta\phi} c / 2\pi f_o \Delta x$$

(Eq. 58)

for $i = 1, 2$. When the two estimates of each are averaged, the standard deviations of the error are reduced by $1/\sqrt{2}$ if $f_{o_i} \approx f_{o_2}$ and $B_1 \approx B_2$.

On the other hand, if coherent temporal processing is used with Eq. 53 to estimate $\cos\psi$ and $\tilde{\beta}_x$, the standard deviations of the error also obey (Eq. 58), with the subscript i set equal to x. In this case the signal-to-noise ratios used to determine $\sigma_{\Delta f_x}$ and $\sigma_{\Delta\tau_x}$ are doubled, which from Eq. 56 again reduces the standard deviations by about $1/\sqrt{2}$ (more for low signal-to-noise ratios). Note the inverse dependence in Eq. 58 on Δx, corresponding to the inverse dependence in Eq. 45 on ΔT.

Suppose, instead, that incoherent temporal processing is used with Eq. 52 to estimate β and β_x and that $f_{o_i} \approx f_{o_2} \approx f_o$ and $\Delta T' = 0$. These latter

assumptions imply that, from the definitions of $\Delta T'$ and $\Delta T''$,

$$-f_{o_1}/k_1 = f_{o_2}/k_2 = \Delta T''/2$$

that, from Eq. 49,

$$\Delta f_1^o \approx \Delta f_2^o \approx \Delta f^o \triangleq \beta_x f_o \Delta x$$

and that, from Eqs. 56 and 57,

$$\sigma_{\Delta f_1} \approx \sigma_{\Delta f_2} \approx \sigma_{\Delta f} \quad .$$

Consider first β_x, since the analysis is easier. From Eq. 52 and the above

$$\tilde{\beta}_x \approx \tilde{\Delta f}^o / f_o \, \Delta x \qquad \text{(Eq. 59)}$$

and hence Eq. 58, with the subscripts dropped, applies. On the other hand, from Eq. 52 and the above,

$$\tilde{\beta} = \frac{(\tilde{\Delta f}_2^o - \tilde{\Delta f}_1^o)}{\Delta T'' \, \beta_x \, \Delta x \, f_o} \qquad \text{(Eq. 60)}$$

and hence

$$\sigma_\beta \approx 2\sigma_{\Delta f} \, / \, [\Delta T'' \, \beta_x \, f_o \, \Delta x] \quad . \qquad \text{(Eq. 61)}$$

6.4 Selection of signal and signal-processing parameters

The same factors govern the selection of signal and signal-processing parameters for coherent spatial processing as they do for coherent temporal processing, with Δx taking the place of ΔT ; hence the comments of Sect. 4.4 apply direct and will not be repeated. Note that if incoherent temporal processing is used they will not be repeated. Note that if incoherent temporal processing is used there will be a conflict in the selection of signal parameters between those that are best for some temporal measurement – large T, small B, and those that are best for other temporal and spatial measurements – small T, large B. Of course such a conflict will not exist if coherent temporal processing if used.

As an example, consider a pulse with f_o = 3500 Hz, B = 217 Hz, and T = 0.5 s, and two hydrophones placed 100 m apart. If the two hydrophones, were 1 m apart then because of the analogy between this chapter and Ch. 4,

Fig. 6a for two such pulses 1 s apart in time would apply direct, with β_x measured in $(km)^{-1}$ corresponding to β in mrad/s, and Fig. 6b would apply with the error standard deviation for $\cos\psi$ found by taking that for $\dot{\ell}$ in knots and dividing by two. Since the hydrophones are 100 m apart, from Eq. 58 the standard deviations of the error are less by a factor of 100 ; therefore β_x and its error standard deviation in (km^{-1}) are found by taking β and its error standard deviation in mrad/s and dividing by 100 and the error standard deviation for $\cos\psi$ is found by taking that for $\dot{\ell}$ in knots and dividing by 200. Suppose that $\psi = 0$, $r_R = 20$ km, and $\gamma \equiv 0$; then from Eq. 50 $\beta_x = 0.2\ km^{-1}$ corresponds to $\tan\alpha = 4$ or $\alpha = 76^o$. An error standard deviation for β_x of 0.005 – not unreasonable in the light of Fig. 6a – corresponds in this case to that for $\tan\alpha$ of 0.1 or at $\alpha = 0$, since the error in α is roughly $\cos^2\alpha$ times the error in $\tan\alpha$, an error standard deviation for α of 0.1 radians $\approx 6^o$. Under the same circumstances, an error standard deviation for $\cos\psi$ of 0.01 – again not unreasonable in the light of Fig. 6b – corresponds to that for ψ of 0.05 rad $\approx 3^o$. Now consider the use of Eq. 52 to measure β .

It follows from Eqs. 58 and 61, that the error standard deviation for β is $2/\Delta T"\ \beta_x$ times that for β_x ; therefore for the pulse and hydrophone pair assumed above the error standard deviation for β in mrad/s is that of Fig. 6a divided by $0.8\ \beta_x$, with β_x given in (km^{-1}). For $\alpha = 45^o$, $\psi = 0$, $r_R = 20$ km, and $\gamma \equiv 0$, $\beta_x = 0.05\ (km^{-1})$ and, from Fig. 6a, an error standard deviation of roughly 12 mrad/s results. As in Ch. 4, for the parameters used it is not possible to improve the estimate of $\cos\psi$ by the use of phase information, because of phase ambiguities; however, if that were possible, the error would be 0.001 rad $\approx 0.06^o$.

7 ALGORITHMS

This chapter looks briefly at how the incoherent and coherent measurement techniques discussed in the previous chapters might be used in practice. The first step required is estimation of the background power, followed by a preliminary single-echo detection. Next, either the incoherent or coherent measurement schemes are applied or, in an even more comprehensive scheme, one of the space/frequency schemes. Finally, the echoes are combined incoherently or coherently, as appropriate, and the final detection decision is made as to whether or not a target is present.

7.1 Estimation of background power

One single way of estimating the background level is by smoothing the matched-filter output power over a suitable interval with a gap in the centre length sufficient to exclude an echo if one occurs there. (If the two FM pulses have the same centre frequency, and hence only one matched filter is used, the presence of two echoes must be appropriately dealt with by using a long enough gap or two gaps.) ALternatively, the noise level may be tracked by a suitable recursive filtering algorithm, such as a Kalman-type filter, with data from detected targets excluded.

7.2 Single-echo detection

Given a running estimate of the noise level using either of the above or any other technique, single-echo detection can be carried out in the standard manner; that is, by smoothing the matched-filter output power over an interval of either T_S or T_F (depending on the type of measurement extraction to be used) followed by comparison with a threshold. The purpose of the preliminary single-ping detection is twofold: first to reduce the amount of data for further processing, and second to ensure that echoes that are processed further have adequate signal-to-noise ratio to make probability of global measurement errors negligible. For this reason the threshold should be set relatively low to ensure a very small probability of measured detection at the expense of a relatively high false-alarm rate. In the final detection, following combination of echoes, a second threshold will be set to reduce the false-alarm rate to acceptable levels. As will be discussed below, it is possible to dispense with this preliminary detection in some versions of the coherent processing scheme.

7.3 Incoherent measurement extraction

The first step in the application of the techniques described in Ch. 3 is an estimation of the echo-plus-background-power level and determination of the half-echo-power times. The accuracy required of the estimate of the echo-plus-background levels was not discussed in Ch. 3 and will be discussed only briefly here. In the first place the background- and echo-power level estimates do not have to be accurate in any absolute sense, but only need to be accurate relative to each other. In the second place the acoustic centre and acoustic length of a target are only loosely tied to the geometric centre and length; therefore a fair error in estimation of the echo-plus-background level would seem tolerable. A simple method of estimating the echo-plus-background level is as follows: once the smoothed matched-filter power exceeds the detection threshold, look ahead by an amount equal to the maximum target length plus T_S. If the smoothed matched-filter power at this point exceeds the detection threshold the target is too long and the echo should be rejected. On the other hand, if this is not true, search back in time to the point where the smoothed matched-filter power exceeds the detection threshold. Next, average the smoothed-matched-filter output power over the interval between the two crossings of the threshold to estimate the echo-plus-signal power. The half-echo-power times may now be estimated by averaging the background and echo-plus-background levels and searching before and after the two detection-level crossings to where the smoothed-matched-filter power drops below the half-echo-power level. Finally, the centre and length of the echo can be estimated by averaging and differencing the half-echo-power times.

This whole procedure is illustrated in Fig. 7.

If both echoes from a target are detected then measurements of ℓ, $\dot{\ell}$, L' and $\dot{L}'$ may be determined from the centres and lengths of the two echoes by using the equations of Sect. 3.1. On the other hand, if only one echo is detected then (assuming $\Delta T' = 0$) estimates of $\ell \pm \dot{\ell}\ (\Delta T + T'')/2$ and $L' \pm \dot{L}'(\Delta T + \Delta T'')/2$ can be obtained by using an obvious modification of the equations of Sect. 3.1. If the two FM pulses have different centre frequencies, it will be known to which pulse the echoes correspond and hence the appropriate sign that applies in these measurements; otherwise this ambiguity is present. Accuracy of the measurements may be estimated by use of the estimated echo-plus-background and background power levels to estimate the signal-to-noise ratios for the echoes and the use of equations of Sects. 3.2 and 3.3 modified in an obvious way to reflect the fact that only one echo is present or, if two echoes are present, that they have different signal-to-noise ratios. (If the two pulses have the same centre frequency it is reasonable to average the two signal-to-noise ratios of the echo; otherwise, it is more reasonable to estimate a σ_{τ_d} and a $\sigma_{\Delta\tau_d}$ for each echo and average the results.)

7.4 Coherent algorithms

If only one echo is detected in the preliminary detection process described in Sect. 7.2, incoherent processing techniques must be used. If two echoes are detected, the next step is cross-correlation of the two echoes in time and frequency. This task may be accomplished as follows. For the second echo, find the maximum in smoothed matched filter output power in the interval T_F after the detection time; a segment of the unsmoothed matched filter output T_F in length and centred on this maximum is used in the cross-correlation. For the first echo, similar segments T_F in length centred $\Delta T + \Delta\tau$ earlier are used for the set of $\Delta\tau$ over which time correlation is sought. For each first-echo segment, the processing is as follows: the first-echo segment is multiplied time by time by the second-echo segment and the result fourier transformed to yield the cross-correlation in frequency between the two segments in frequency. The resulting set of frequency cross-correlations is the required time and frequency cross-correlation between the first and second echo, which may be processed as described in Sect. 4.2 to yield the time and frequency shifts of the peak, from which $\dot{\ell}$ and β may be estimated by using the equations of Sect. 4.1.

To estimate ℓ and L', incoherent processing must be used. To that end, segments of suitable length centred on the two echoes are added coherently; for this process the segment containing the first echo must be centred on a time $\Delta T + \tilde{\Delta\tau}^{o}$ earlier than the centre of the segment containing the second echo and must be shifted up in frequency by $\tilde{\Delta f}^{o}$ and rotated in phase by $\tilde{\Delta\phi}^{o}$. It is convenient if the result of the coherent addition is halved so that the final result has the same background level as the original echo. This result is then smoothed over an interval T_s, processed as in Sect. 7.3

to find its centre and length, and equations of Sect. 4.1 used to estimate ℓ and L'. Accuracy of the estimates $\dot{\ell}$, $\dot{\beta}$, ℓ and L may be obtained using the equations of Sects. 3.2, 4.2, and 4.3, taking note of the comments made in Sect. 7.3 on the subject of measurement accuracy.

7.5 Space/frequency algorighms

For each hydrophone the background level is determined as in Sect. 7.1 and the two results averaged (unless there is some reason to believe that the background levels of the two hydrophones will differ). Next, the single-ping detection schemes are applied to the output of each hydrophone. If only one echo is detected the incoherent processing of Sect. 7.3 must be used and $\cos\psi$ and β_x cannot be estimated. If only two echoes are detected and both are on the same hydrophone, then either incoherent processing as in Sect. 7.3 or coherent processing as in Sect. 7.4 is used, as appropriate, and again $\cos\psi$ and β_x cannot be estimated. If two echoes are present on different hydrophones and it is known that they come from the same pulse then incoherent space/frequency processing with suitable and obvious modification can be used to obtain a reduced set of measurements ($\dot{\ell}$ and L' cannot be estimated); otherwise ordinary incoherent processing may be applied to each hydrophone and the measurements so obtained averaged (in which case $\dot{\ell}$, L', $\cos\psi$ and β_x cannot be estimated). If three echoes are present and it is known which echo is missing, either incoherent or coherent space/frequency processing can be used as appropriate, with, however, suitable and obvious modification for the missing echo. If three echoes are present and it is not known which echo is missing, the output of each hydrophone must be processed individually and the measurements from the two hydrophones appropriately averaged (in which case $\cos\psi$ and β_x cannot be estimated).

The most interesting case is of course when all four echoes — two on each hydrophone — are detected. Then the principles of Ch. 5 can be used to obtain estimates of ℓ, $\dot{\ell}$, L, L' or β_x. The procedures to be carried out should be obvious from the discussions of Ch. 5 and Sects. 7.3 and 7.4 and will not be belaboured here.

7.6 Multiple-echo detection

Multiple-echo detection is in principle no different from single-echo detection, except that the echoes are added together either incoherently or coherently prior to comparison with a threshold. In the case of incoherent processing the matched-filter output power for the first echo suitably shifted in time is added to that for the second and then smoothed over an appropriate interval prior to the comparison. In the case of coherent processing the matched filter output for the first echo suitably shifted in time, frequency, and phase is added to that for the second and then magnitude squared and smoothed prior to the comparison. If the smoothing interval is T_F, which is a reasonable choice, a short cut can be used to obtain the result: add

twice the magnitude of the correlation peak squared to the two maxima of the smoothed output power used to make the preliminary detection of the two echoes. Alternatively, pre-detection can be avoided entirely if the matched-filter output power is smoothed over an interval of T_F and at the same time a running correlation in time and frequency, such as described in Sect. 7.3, is made between the match-filter output at a given time and a time ΔT sooner and added to twice the maximum of the magnitude squared of the double correlation for the given time, and comparing it to a threshold. Once a detection is made, the techniques of Sect. 7.3 are used to estimate target properties.

Multiple-echo detection for the space/frequency algorithms is similar to that just described. If incoherent processing is used, for each pulse in the ping, the two echoes from the two hydrophones are added coherently and the results for the two pulses are then added incoherently. The spatial analogue of the temporal processing just described can be used to perform the coherent addition and even to perform preliminary detection for echoes from each pulse. If coherent space/frequency processing is used, the four echoes may be added coherently by the following spatial/temporal analogue of the temporal processing just presented. The matched filter output powers for the two hydrophones are added and smoothed over an interval of T_F.

At the same time a running, temporal, double correlation is made for each hydrophone between pulses, the results added, and the maximum magnitude squared found. Similarly, running spatial double correlations are made for each pulse between hydrophones, summed, and the maximum magnitude squared found. Finally, two more running double correlations are made between differing pulses on differing hydrophones and the maximum magnitudes found. The smoothed power in the coherent sum of the four echoes at a given time is the sum of the smoothed, summed, matched-filter output powers at that time, the same at a delay of ΔT, and twice the sum of all the double correlation maxima.

CONCLUSIONS

With the use of a double FM pulse it is possible to measure ℓ, $\dot{\ell}$, L and $\dot{L}$ or β for a long, thin target such as a submarine. These quantities may be measured using incoherent processing of the echoes, in which case the best signal to transmit is the roof top FM where $f_{o_1}/k_1 \approx -f_{o_2}/k_2$; furthermore, processing is eased if f_{o_1} is taken different from f_{o_2} so that the two echoes may be clearly identified. In general, to measure ℓ and L well a relatively short pulse of large bandwidth should be used; while to measure $\dot{\ell}$ and $\dot{L}$ well a relatively long pulse of small bandwidth is preferable. The quantities $\dot{\ell}$ and $\dot{L}$ can be measured using coherent processing of the echoes, in which case the best signal to transmit consists of two identical FM pulses of relatively short time and long bandwidth. Incoherent processing does relatively better in measuring $\dot{\ell}$,

while coherent processing does better in measuring β. Use of phase information in the coherent processing can significantly improve $\dot{\ell}$ measurement if phase ambiguities can be avoided. With the use of a double FM pulse and two hydrophones it is possible to measure, in addition, $\cos\psi$ and β_x. The temporal processing may be either incoherent or coherent, but spatial processing must be coherent. The best signal to use is determined by the type of temporal processing to be used. Again, use of phase information presents the possibility of significantly improving $\cos\psi$ measurement if phase ambiguities can be avoided. By incoherent and coherent combination of the echoes received on either one or two hydrophones, detection performance may be significantly improved.

The analysis of this report assumes that an ordinary, linear FM pulse and only a filter matched to it are used. As a result, there is a limit on the resolution attainable for targets with large $|\dot{\ell}|$. This limitation may be avoided in one of two ways: use of the doppler-invariant FM signal or use of a bank of matched filters. With either approach, resolution may be improved at will be using a wider bandwidth signal. These procedures might be of use if coherent processing is to be employed, as performance may then be limited by bandwidth. Most of the analysis contained herein applies if either of the resolution-improving schemes is employed, provided that the correct expression for resolution is used; however, some of the doppler correction terms may be modified or eliminated.

Much work remains to be done in this area. In the first place the equations contained herein for the standard deviations of the measurement error should be verified by simulation and sea trials. (Some verification of the measurement of $\dot{\ell}$ with sea-trial data has been carried out by Plaisant *[10]*, who indicates that his equations and the extensions contained herein may be optimistic.) A second area of major interest is the effect of time and frequency spreading on measurement errors. Finally, the question of what the measurement procedures will yield for targets that are not long, thin, and rigid is of interest since false targets may in fact not be of that form. The theory contained in *[6]* provides the basis for analyzing the effects of the medium and the target on the measurement processes.

One type of dispersive medium that can be analyzed with little further work is a medium that spreads the signal in time only. In this case the echo is simply what would be obtained without the spreading, convolved with the time-spreading of the medium. For example, suppose that the medium contains multipaths, then if coherent temporal processing is employed, the double correlation must be convolved with the autocorrelation function of the multipath structure along the time axis. If the multipath delays are large compared with the width of the double correlation peak in time, the techniques described herein may be used to determine the autocorrelation function of the multipath structure. If the multipath structure could be inferred from its autocorrelation, then incoherent processing to measure ℓ and L and detection performance could be greatly improved by convolution of the matched-filter outputs with the multipath structure. Unfortunately, a given autocorrelation function will not correspond to a unique multipath structure. One possibility is to convolve the matched-filter output with all multipath structures consistent with the measured autocorrelation of the multipath structure to see which gives maximum output. These processes seem worthy of further study.

REFERENCES

1. HEERING, P. de Modelling and detection. In: TACCONI, G. ed. Aspects of Signal Processing with Emphasis on Underwater Acoustics. Proceedings of the NATO Advanced Study Institute held at Portovenere, La Spezia, Italy, 30 August-11 September, 1976. Dordrecht, The netherlands, Reidel, 1977: 181-201.

2. MEIER, L. A resume of stochastic, time-varying, linear system theory with applications to active-sonar signal-processing problems. SACLANTCEN SR-50. La Spezia, Italy, SACLANT ASW Research Centre, 1981.

3. NATO, SACLANT ASW RESEARCH CENTRE. Bibliography, technical reports, technical memoranda and special reports 1959-1973, SACLANTCEN SB-1, NATO CONFIDENTIAL. La Spezia, Italy, SACLANT ASW Research Centre, 1974.

4. NATO, SACLANT ASW RESEARCH CENTRE. Bibliography, SACLANTCEN reports, 1973- , SACLANTCEN memoranda, 1973- , conférence proceedings, 1971- . SACLANTCEN SB-2, NATO CONFIDENTIAL. La Spezia, Italy, SACLANT ASW Research Centre, 1975.

5. ROSS, D. Twenty years of research at the SACLANT ASW Research Centre 1959-1979, SACLANTCEN M-93, NATO CONFIDENTIAL. La Spezia, Italy, SACLANT ASW Research Centre, 1980.

6. MEIER, L. A resume of deterministic time-varying linear system theory with application to active sonar signal processing problems, SACLANTCEN SR-44, La Spezia, Italy, SACLANT ASW Research Centre, 1980.

7. MEIER, L. Measurement of target characteristics by double FM pulses. In: 1977 Papers presented to the 31st meeting of the SACLANTCEN Scientific Committee of National Representatives, 18-20 October, 1977, SACLANTCEN CP-21, NATO CONFIDENTIAL. La Spezia, Italy, SACLANT ASW Research Centre, 1977: 15/1 - 15/5. [AD C 140 36]

8. KRAMER, S.A. Doppler and acceleration tolerances of high-gain, wideband linear FM correlation sonars. Proceedings of the IEEE, 55, 1967: 627-636.

9. PLAISANT, A. Error model for some submarine target parameters in noisy non-dispersive channels. SACLANTCEN SM-87, NATO RESTRICTED. La Spezia, Italy, SACLANT ASW Research Centre, 1976. [AD C 950 355]

10. PLAISANT, A. Measurement accuracy of some target parameters. In: VETTORI, G. and HUG, E., eds. Submarine echo properties. Proceedings of a conference held at SACLANTCEN, on 10-14 November 1975, SACLANTCEN CP-18: Part 1, NATO CONFIDENTIAL. La Spezia, Italy, SACLANT ASW Research Centre, 1976: 10/1-10/15. [AD C 950 346 Pt. 1]

11. WIEKHORST, F. A study on active acoustic target classification, SACLANTCEN TR-49, NATO CONFIDENTIAL. La Spezia, Italy, SACLANT ASW Research Centre, 1965. [AD 366 229]

12. SEYNAEVE, R. and VAN MARLE, J.C. The space/frequency classification of submarines using a single transducer, SACLANTCEN TR-194, NATO CONFIDENTIAL. La Spezia, Italy, SACLANT ASW Research Centre, 1971. [AD 517 608]

13. HUG, E. Some extensions of the space-frequency classification technique, SACLANTCEN TM-122, NATO RESTRICTED. La Spezia, Italy. SACLANT ASW Research Centre, 1967. [AD A 067 257]

14. HUG, E. and HEERING, P. de Double-pulse methods for active sonar tracking and classification, SACLANTCEN SR-14, NATO CONFIDENTIAL. La Spezia, Italy. SACLANT ASW Research Centre, 1976. [AD C 950 488]

15. DUNSIGER, A.D. Broadband submarine echo properties relevant to sonar detection, SACLANTCEN SM-63, NATO CONFIDENTIAL. La Spezia, Italy. SACLANT ASW Research Centre, 1975. [AD C 950 094]

16. RIHACZEK, A.W. Principles of high-resolution radar, McGraw-Hill, 1969: 287-329.

APPENDICES

APPENDIX A

SPREAD OF DOPPLER AMBIGUITY FUNCTION IN TIME

The purpose of this appendix is to find a reasonable approximation to the spread of $|\gamma^M_{FM}|^2$ in z that is valid for large $|xy|$. The fourier transformation of $|\gamma^M_{FM}|^2$ with respect to z was given in *[6]* of the Main Text as

$$\tfrac{1}{2}\,\sqcap(y/x;1)\sqcap(w,\,1-|y/x|)\,(1-|y/x|-|w|)\,\mathrm{sinc}[2\pi xy(1-|y/x|-|w|)w]\ . \qquad \text{(Eq. A.1)}$$

If the term $|w|$ could be dropped from the sinc function and the factor proceding it, inverse transformation would be easy, and in fact dropping $|w|$ leads to the inadequate approximation for the spread of $|\gamma^M_{FM}|^2$ for large $|xy|$ given in *[6]*. When $|w|$ is dropped, $|\gamma^M_{FM}|^2$ is a rectangular function whose width is the reciprocal of the value of w that yields π for the argument of the sinc function. To obtain a better approximation it is assumed that the spread of $|\gamma^M_{FM}|^2$ is the reciprocal of the value of w that yields π for the argument of the sinc function — this time including one half of the $|w|$ term (inclusion of the full $|w|$ term leads to an unacceptable approximation). The value of w sought must obey (sinc w is positive).

$$\tfrac{1}{2}\,w^2-(1-|y/x|)\,w + 1/(2|xy|) \qquad \text{(Eq. A.2)}$$

therefore it is

$$w = 1-|y/x| - \sqrt{(1-|y/x|)^2 - 1/|xy|}$$

$$= (|x|-|y|)(1-\sqrt{1-|x|/[(|x|-|y|)^2|y|]}/|x| \qquad \text{(Eq. A.3)}$$

since the smallest root is obviously the one sought. Inversion of this result yields the approximation given in the body of the text.

APPENDIX B

DETERMINATION OF THE DOPPLER SHIFT CAUSING THE PEAK MATCHED-FILTER OUTPUT POWER TO FALL BY HALF

Figure 4 of the main text was generated as follows: From Eq. 14 of *[6]* of the main text it follows that we are seeking the value of $|y|$ for which

$$C(b)^2 + S(b)^2 = 0.5|xy|$$

$$b = \sqrt{|xy|}\,(1-|y/x|) \qquad \text{(Eq. B.1)}$$

since for $z = 0$, $a = -b$ and $C(\ )$ and $S(\ )$ are odd functions. By selecting values of b and solving these equations, $y^*(|x|)$ is readily generated.

APPENDIX C

STANDARD DEVIATION OF THE HALF-ECHO-POWER POINTS

This appendix is concerned with Plaisant's approach to determining the time shift and spread of the target echo for an FM pulse by determining the times at which smoothed matched-filter output power crosses a level half way between the full-signal and no-signal levels. Four cases are to be considered, depending on the relationship between the apparent target length (measured in time), the averaging interval, and the spread of $|\gamma^M_{FM_i}|^2$. In all four cases the standard deviation of the error in measuring this time is found by dividing the standard deviation of the smoothed-matched-filter output power at this time by the slope of the expected smoothed-matched-filter output power at this time.

C.1 Case 1 Spread of $|\gamma^M_{FM}|^2$ less than both apparent target length and averaging interval

In this case the convolution with $|\gamma^M_{FM_i}|^2$ in Eq. 21 may be removed and replaced by its integral over τ, which is readily found: from Eq. 14 the integral of $|\gamma^M_{FM_i}|^2$ over z is $(B_i - |\alpha_o - 1| f_{o_i})/B_i$; the integral over τ is just B_i times smaller, or $(B_i - |\alpha_o - 1| f_{o_i})/B_i^2$. The signal-to-noise ratio is found by taking the ratio of the maximum of Eq. 21 to its minimum and is, since the maximum of Eq. 21 occurs when the target is centred in the smoothing interval,

$$\{[\sigma^2_{e_i}(B_i - |\alpha_o - 1| f_{o_i})/B_i^2]/T_i^{**}\}/\sigma_n^2 \quad , \qquad \text{(Eq. C.1)}$$

where T_i^{**} is the larger of T_{s_i} and $\Delta\tau_{d_i}$. This result is identical to that given in the main body after Eq. 22 and is valid also as long as at least either T_{s_i} or $\Delta\tau_{d_i}$ is larger than the spread of $|\gamma^M_{FM_i}|^2$ – i.e. also for the next two cases. Since the expected smoothed echo power is,

from Eq. 21, equal to

$$A = \frac{\sigma_{e_i}^2 \, (B_i - |\alpha_o - 1| f_{o_i})}{B_i^2 \, T_{s_i} \, \Delta\tau_{d_i}} \qquad \text{(Eq. C.2)}$$

times the convolution between two ⌐¬ functions, its derivative at the half-echo power point is just A.

Calculation of the standard deviation of the half-signal-power point is harder. The smoothed power at this point consists of $1/T_{s_i}$ times the sum of two uncorrelated signals (see *[9]* of the main text): the integral over $T_i^*/2$ of echo-plus-noise and the integral of $T_{s_i} - T_i^*/2$ of noise alone. Because the noise is a band-limited, gaussian, white noise with power σ_n^2 and bandwidth B_i, the latter integral is proportional to a chi-squared variable with $2\,B_i(T_{s_i} - T_i^*/2)$ degrees of freedom; hence its variance is $\sigma_n^2(T_{s_i} - T_i^*/2)/B_i$. For no doppler the first integral is also readily evaluated because the echo-plus-noise is again band-limited, gaussian, white noise with bandwidth B_i, but with power $\sigma_n^2 + \sigma_{e_i}^2/B_i\Delta\tau_{d_i}$; the result is a variance of $(\sigma_n^2 + \sigma_{e_i}^2/B_i\,\Delta\tau_{d_i})^2(T_i^*/2)/B_i$. Adding these two, taking the square root, and dividing by T_{s_i}, yields a standard deviation of smoothed power at the half-signal power point of

$$\sqrt{\frac{1}{2B_i \, T_{s_i}^2} \left[(\sigma_{e_i}^2/B_i \, \Delta\tau_{d_i})^2 \, T_i^* + 2(\sigma_{e_i}^2/B_i\Delta\tau_{d_i}) \, \sigma_n^2 T_i^* + 2\sigma_n^4 \, T_{s_i}\right]} \qquad \text{(Eq. C.3)}$$

which is Plaisant's result.

Unfortunately, for non-zero doppler shift, the echo no longer has bandwidth B_i and the first integral is more difficult to compute. What is required is the variance of

$$\int_0^{T_i^*/2} |x_1(\tau) + x_2(\tau)|^2 d\tau = \int_0^{T_i^*/2} |x_1(\tau)|^2 d\tau + \int_0^{T_i^*/2} 2\mathrm{Re}[x_1^*(\tau)x_2(\tau)]d\tau + \int_0^{T_i^*/2} |x_2(\tau)|^2 d\tau$$

(Eq. C.4)

where $R_e[\ ]$ indicates "real part of" and x_1 and x_2 are independent, band-limited, gaussian noises of powers σ_n^2 and $\sigma_{e_i}^2 (B_i - |\alpha_o - 1| f_{o_i}) B_i^2 \Delta\tau_{d_i}$ respectively and bandwidths B_i and $B_i - |\alpha_o - 1| f_{o_i}$ respectively. Because of the independence of x_1 and x_2, the three integrals on the right hand of Eq. C.4 are uncorrelated; hence the variance of the integral on the left is the sum of the variances of the three on the right. The variances of the first and third integrals are readily found to be $\sigma_n^4 T_i^*/(2B_i)$ and $\sigma_{e_i}^4 (B_i - 2\alpha_o - 1| f_{o_i}) T_i^*/(2B_i^4 \Delta\tau_{d_i}^2)$, respectively. Since $x_1(\tau)$ and $x_2(\tau)$ are independent, the expected value of the second integral is zero and its variance equals the expected value of its magnitude squared i.e.

$$\int_{-T_i^*/2}^{T_i^*/2} \int_{-T_i^*/2}^{T_i^*/2} E\{[x_1^*(\tau)x_2(\tau) + x_1(\tau)x_2^*(\tau)]^*[x_1^*(\sigma)x_2(\sigma) + x_1(\sigma)x_2^*(\sigma)]\} d\tau d\sigma$$

$$= 2 \int_{-T_i^*/2}^{T_i^*/2} \int_{-T_i^*/2}^{T_i^*/2} \mathrm{Re}\, E[x_1(\tau)x_1^*(\sigma)]\, E[x_2^*(\tau)x_2(\sigma)] d\tau d\sigma$$

$$= 2[\sigma_n^2 \sigma_{e_i}^2 (B_i - |\alpha_o - 1| f_{o_i})/B_i^2 \Delta\tau_{d_i}] \int_{-T_i^*/2}^{T_i^*/2} \int_{-T_i^*/2}^{T_i^*/2} \mathrm{sinc}[\pi(B_i - |\alpha_o - 1| f_{o_i})(\tau - \sigma)]$$

$$\mathrm{sinc}[\pi B_i(\tau - \sigma)] d\tau d\sigma$$

$$\approx 2[\sigma_n^2 \sigma_{e_i}^2 (B_i - |\alpha_o - 1| f_{o_i}) T_i^*/B_i^2 \Delta\tau_{d_i}] \int_{-\infty}^{\infty} \mathrm{sinc}[\pi(B_i - |\alpha_o - 1| f_{o_i})\tau]\, \mathrm{sinc}(\pi B_i \tau) d\tau$$

$$= 2\, \sigma_n^2 \sigma_{e_i}^2 (B_i - |\alpha_o - 1| f_{o_i})\, T_i^*/B_i^3 \Delta\tau_{d_i}\ , \qquad \text{[Eq. C.5]}$$

which, when added to the two other portions of the echo-plus-noise variance and the noise-only variance, yields for the standard deviation at the half-signal power point:

$$\sqrt{\frac{1}{2B_i\ T_{s_i}^2}\left[(\sigma_{e_i}^2/B_i\ \Delta\tau_{d_i})^2\left(\frac{B_i-|\alpha_o-1|f_{o_i}}{B_i}\right)T_i^* + 2\ \sigma_n^2(\sigma_{e_i}^2/B_i\ \Delta\tau_{d_i})\left(\frac{B_i-|\alpha_o-1|f_{o_i}}{B_i}\right)T_i^* + 2\sigma_n^4\ T_{s_i}\right]} \quad \text{(Eq. C.6)}$$

Division of this result by A and use of the definition of S/N yields (Eq. 22).

C.2 Case 2 Spread of $|\gamma_{FM}^M|^2$ more than apparent target length but less than averaging interval

In this case the factor in the double convolution (Eq. 21) corresponding to the target can be dropped; therefore the slope at the half signal-power-point is

$$\frac{\sigma_{e_i}^2}{T_{s_i}}\ |\gamma_{FM_i}^M(0,\ \alpha_{o_i})|^2 \quad . \qquad \text{(Eq. C.7)}$$

Since the variance is due to noise only, the standard deviation of smoothed power is readily determined to be

$$\sigma_n^2/\sqrt{B_i\ T_{s_i}} \quad . \qquad \text{(Eq. C.8)}$$

Division of the latter by the former and use of the definition of signal-to-noise ratio yields (Eq. 23).

C.3 Case 3 Spread of $|\gamma^M_{FM}|^2$ less than apparent target length and no smoothing

In this case the factor in the double convolution (Eq. 21) corresponding to the moving average smoothing can be dropped; therefore the slope at the half-signal-power point is

$$\frac{\sigma^2_{e_i}}{\Delta\tau_{d_i}} |\gamma^M_{FM_i}(0, \alpha_{o_i})|^2 \quad . \qquad \text{(Eq. C.9)}$$

Since T_{s_i} is assumed to be less than $1/B_i$, the variation in smoothed power about its mean is proportional to a chi-squared variable with two degrees of freedom. At the half-signal-power point the expected echo power is, by definition, one half of the maximum expected echo power; hence the standard deviation of the smoothed power is

$$(1/2\ S/N_i + 1)\ \sigma^2_n \quad . \qquad \text{(Eq. C.10)}$$

Division of this result by the slope and use of the definition of signal-to-noise ratio yields (Eq. 24).

C.4 Case 4 Spread of $|\gamma^M_{FM}|^2$ more than apparent target length and no smoothing

In this case both the factor in the double convolution (Eq. 21) corresponding to the moving average and that corresponding to the target may be dropped. The peak signal-to-noise ratio is then S/N_i, as given following (Eq. 25), and the half echo-power points occur when $|\gamma^M_{FM_i}(\tau, \alpha_o)|^2$ equals one-half. Let τ^*_i be the negative value of τ for which this occurs; the corresponding slope is just $\sigma^2_{e_i}$ times the derivative of $|\gamma^M_{FM_i}(\tau, \alpha_o)|^2$ at τ^*_i. Furthermore, the variation of the power due to noise alone is just σ^2_n. Use of these results yields (Eq. 25).

APPENDIX D

STANDARD DEVIATION OF THE 50% CORRELATION POINTS

This appendix is concerned with Plaisant's approach to determining the position of the correlation peak in time and frequency between the two echoes from a double FM pulse by determining the times and frequencies at which the magnitude of correlation is half of the maximum. In analogy with Appendix C, standard deviations of the half-correlation-peak points are determined by dividing the standard deviation in the magnitude of correlation by the slope of the expected magnitude of correlation at the half-peak point on the expected magnitude of correlation. Correlation between the time and frequency points is ignored. In addition, measurement of phase at the peak is treated.

D.1 Correlation in frequency

From the discussion of Sect. 4.1 of the main text it is clear that, for $\Delta\tau = \Delta\tau^{o}$, the correlation in frequency, if normalized and shifted in frequency so the peak is at the origin, is the correlation $Y(f)$ between $X(f) = \mathcal{F}[x(\tau)]$ and $X'(f) = \mathcal{F}[x'(\tau)]$, where

$$x(\tau) \triangleq [\gamma(\tau) \otimes h(\tau) + n(\tau)] \sqcap(\tau;\, T_F/2)/\sqrt{T_F}\ ,$$

$$x'(\tau) \triangleq [\gamma'(\tau) \otimes h(\tau) + n'(\tau)] \sqcap(\tau;\, T_F/2)/\sqrt{T_F}\ , \qquad \text{(Eq. D.1)}$$

$h(\tau)$ is a segment of gaussian white noise of length $\Delta\tau_d$ centred on the origin and of power $\sigma_e^2/\Delta\tau_d$; $n(\tau)$, and $n'(\tau)$ are uncorrelated, gaussian, white noises of power σ_n^2 ; $\gamma'(\tau)$ is $\gamma^{M}_{FM}(\tau,\alpha_o)$; and $\gamma(\tau)$ is the inverse fourier transform of $\Gamma^{M}_{FM}(f,\alpha_o)$ with its frequency limits shifted up by Δf_o . Thus $|E[Y(f)]| \approx E[|Y(f)|]$ is sought to determine the frequency and slope of the half-correlation-peak points, $\text{var}\,[Y(f)]/2 \approx \text{var}\,|Y(f)|$ is sought to find the variance at the half-correlation-peak, and

$$\text{cov}\,[Y^*(-f)\, Y(f)]/2 \approx \text{cov}(|Y(-f)|\ |Y(f)|)$$

to find their correlations.

The inverse fourier transform of $Y(f)$ is

$$y(\tau) = x^*(\tau)\, x'(\tau) \quad ; \qquad \text{(Eq. D.2)}$$

therefore, since $n(\tau)$ and $n'(\tau)$ are independent

$$E[y(\tau)] = E\{[\gamma(\tau) \underset{\tau}{\circledast} h(\tau)]^*[\gamma'(\tau) \underset{\tau}{\circledast} h(\tau)]\} \sqcap(\tau, T_F/2)/T_F$$

$$= \sqcap(\tau; T_F/2)/T_F \int_{-\infty}^{\infty}\int_{-\infty}^{\infty} \gamma^*(\tau-\sigma)\gamma'(\tau-\sigma')h^*(\sigma)h(\sigma')\, d\sigma d\sigma'$$

$$= \frac{\sigma_e^2 \sqcap(\tau; T_F/2)}{\Delta\tau_d\, T_F} \int_{-\Delta\tau_d/2}^{\Delta\tau_d/2} \gamma^*(\tau-\sigma)\, \gamma'(\tau-\sigma)\, d\sigma$$

$$\approx \frac{\sigma_e^2 \sqcap(\tau; T^*/2)}{\Delta\tau_d\, T_F} \int_{-\infty}^{\infty} \gamma^*(\sigma)\, \gamma'(\sigma)\, d\sigma$$

$$= \frac{\sigma_e^2 \sqcap(\tau; T^*/2)}{\Delta\tau_d\, T_F} \int_{-\infty}^{\infty} \Gamma^*(f)\, \Gamma'(f)\, df$$

$$= \frac{\sigma_e^2 \sqcap(\tau; T^*/2)}{B^2\, \Delta\tau_d\, T_F} \int_{-\infty}^{\infty} \sqcap(f-\Delta f^o; B-|\alpha_o-1|f_o) \sqcap(f; B-|\alpha_o-1|f_o)\, df$$

$$= \frac{\sigma_e^2 (B-|\alpha_o-1|f_o-|\Delta f^o|)}{B^2\, T_F} \sqcap(\tau; T^*/2)$$

$$= S/N\, \sigma_n^2\, \frac{(B-|\alpha_o-1|f_o-|\Delta f^o|)}{(B-|\alpha_o-1|f_o)\, T^*} \sqcap(\tau; T^*/2) \qquad \text{(Eq. D.3)}$$

if the spread of $|\gamma|$ $|\gamma'|$ is small compared with T^* . But $|\gamma'| = |\gamma^M_{FM}|$ and $|\gamma|$ is just $|\gamma^M_{FM}|$ time shifted; thus the spread of $|\gamma|$ $|\gamma'|$ is roughly the spread of $|\gamma^M_{FM}|$ and will be small compared with T^* if the spread of $|\gamma^M_{FM}|$ is small. The magnitude of the fourier transform of $E[y(\tau)]$ is

$$|\mathcal{F}[E(y(\tau))]| = |E[Y(f)]| \approx E[|Y(f)|]$$

$$\approx S/N\ \sigma_n^2[(B-|\alpha_o-1|f_o-|\Delta f^o|)/(B-|\alpha_o-1|f_o)]\mathrm{sinc}(\pi\ f\ T^*)\ .$$

(Eq. D.4)

The sinc function is 50% of its peak value at $f = \pm\ 0.6\ \pi$; therefore $E[Y(f)]$ has 50% of its peak value at $f = \pm\ 0.6/T^*$. The slope at $f = -\ 0.6/T^*$ is:

$$0.43\ \pi\ T^*\ S/N\ \sigma_n^2(B-|\alpha_o-1|f_o-|\Delta f^o|)/(B-|\alpha_o-1|f_o) \qquad \text{(Eq. D.5)}$$

From the above it is clear that if the spread of $|\gamma^M_{FM}|^2$ is less than T^*, the echo portion of the matched filter otuput for each of the FM pulses is a segment T^* in length of band-limited, gaussian, white noise of bandwidth $B-|\alpha_o-1|f_o$, the bandwidth of $\Gamma^M_{FM}(f,\alpha_o)$, while the noise portion is a segment T_F in length of gaussian white noise of bandwidth B :

$$x(\tau) \approx [h'(\tau) \sqcap (\tau;T^*/2) + n(\tau) \sqcap (\tau;T_F/2)]/\sqrt{T_F}$$

$$x'(\tau) \approx [h''(\tau) \sqcap (\tau;T^*/2) + n'(\tau) \sqcap (\tau;T_F/2)]/\sqrt{T_F}$$

$$y(\tau) \approx \{[h'^*(\tau)h''(\tau) + h'^*(\tau)n'(\tau)+n^*(\tau)h''(\tau)] \sqcap (\tau;T^*/2)$$

$$+ n^*(\tau)n'(\tau) \sqcap (\tau;T_F/2)\}\ /T_F .$$

(Eq. D.6)

The centre frequencies are $f_o' + \Delta f^o$, $f_o - \Delta f^o$, f_o' and f_o respectively for $h'(\tau)$, $n(\tau)$, $h''(\tau)$ and $n'(\tau)$. From the discussion in the main test $E[|Y(f)| - |Y_e(f)|]^2$ and $E\{[|Y(-f)| - |Y_e(-f)|]\,[Y(f) - |Y_e(f)|]\}$ are sought where

$$Y_e(f) = \mathcal{F}[y_e(\tau)] ,$$

$$y_e(\tau) = h'^*(\tau)\, h''(\tau) \sqcap(\tau, T^*/2) . \qquad \text{(Eq. D.7)}$$

If, as is assumed, $|Y_e(f)|$ is large compared with $|Y(f)| - |Y_e(f)|$, then $|Y(f)| - |Y_e(f)|$ is approximately the variation of $Y(f)$ along the direction of $Y_e(f)$:

$$|Y(f)| - |Y_e(f)| \approx \mathrm{Re}[e^{-j\phi}\delta Y(f)] , \qquad \text{(Eq. D.8)}$$

where ϕ is the argument of $Y_e(f)$ and $\delta Y(f) = Y(f) - Y_e(f)$. Furthermore, since $Y_e(-f) \approx Y_e^*(f)$,

$$|Y(-f)| - |Y_e(-f)| \approx \mathrm{Re}[e^{+j\phi}\delta Y(-f)] . \qquad \text{(Eq. D.9)}$$

Let $\delta Y(f)$ have real and imaginary parts $\delta Y_R(f)$ and $\delta Y_I(f)$; then

$$E[|\delta Y(f)|^2] = E\{[\delta Y_R(f)]^2\} + E\{[\delta Y_I(f)]^2\} ,$$

$$E\{[\delta Y(f)]^2\} = E\{[\delta Y_R(f)]^2\} - E\{[\delta Y_I(f)]^2\} + 2j\, E\{\delta Y_R(f)\, \delta Y_I(f)\} ,$$

$$E\{\mathrm{Re}[e^{-j\phi}\delta Y(f)]\} = E\{[\delta Y_R(f)\cos\phi + \delta Y_I(f)\sin\phi]^2\}$$

$$= 1/2\, E[|\delta Y(f)|^2]$$

(Eq. D.10)

if $E\{[\delta Y(f)]^2\} = 0$. Furthermore

$$E[\delta Y^*(-f)\ \delta Y(f)] = E[\delta Y_R(-f)\ \delta Y_R(f)] + E[\delta Y_I(-f)\ \delta Y_I(f)] - j\ E[\delta Y_R(-f)\ \delta Y_I(f) - \delta Y_I(-f)\ \delta Y_R(f)]$$

$$E[\delta Y(-f)\ \delta Y(f)] = E[\delta Y_R(-f)\ \delta Y_R(f)] - E[\delta Y_I(-f)\ \delta Y_I(f)] - j\ E[\delta Y_R(-f)\ \delta Y_I(f) + \delta Y_I(-f)\ \delta Y_R(f)]$$

$$E\{Re[e^{+j\phi}\delta Y(-f)]\ Re[e^{-j\phi}\delta Y(f)]\} = E\{[Y_R(-f)\cos\phi - Y_I(-f)\sin\phi]\ [Y_R(f)\cos\phi + Y(f)\sin\phi]\} = 0$$

(Eq. D.11)

if $E[\delta Y^*(-f)\ \delta Y(f)] = E[\delta Y(-f)\ \delta Y(f)]$.

From the properties of the fourier transform, the inverse transforms of $|\delta Y(f)|^2$, $\delta Y(f)^2$, $\delta Y^*(-f)\ \delta Y(f)$, $\delta Y(-f)\ \delta Y(f)$ obey

$$\mathcal{F}^{-1}[|\delta Y(f)|^2] = \delta y^*(-\tau) \times \delta y(\tau) \ ,$$

$$\mathcal{F}^{-1}[\delta Y(f)^2] = \delta y(\tau) \times \delta y(\tau) \ ,$$

$$\mathcal{F}^{-1}[\delta^* Y(-f)\ \delta Y(f)] = \delta y^*(\tau) \times \delta y(\tau) \ ,$$

$$\mathcal{F}^{-1}[\delta Y(-f)\ \delta Y(f)] = \delta y(-\tau) \times \delta y(\tau) \ ,$$

(Eq. D.12)

where $\delta(\tau) = y(\tau) - y_e(\tau)$; therefore we need to evaluate the expected values of these four convolutions and show that it is zero for the last three. The second and last convolution clearly have zero expectations since they are sums of terms such as

$$E[h'^*(\tau \pm \sigma)\ h'^*(\sigma)]\ E[n'(\tau \pm \sigma)\ n'(\sigma)] \ ,$$

which are zero. On the other hand, since $h'(\tau)$, $h''(\tau)$ and $n'(\tau)$ are uncorrelated:

$$E[y^*(-\tau) \times y(\tau)] \approx A(\tau) + B(\tau) + C(\tau)$$

$$E[y^*(\tau) \times y(\tau)] \approx A'(\tau) + B'(\tau) + C'(\tau)$$

where (Eq. D.13)

$$A(\tau) = E\{[n^*(-\tau)\, h''(-\tau) \sqcap\!\sqcup (\tau;T^*/2)]^* \underset{\tau}{\otimes} [n^*(\tau)\, h''(\tau) \sqcap\!\sqcup (\tau;T^*/2)]\}/T_F^2 \ ,$$

$$A'(\tau) = E\{[n(\tau)\, h''(\tau) \sqcap\!\sqcup (\tau;T^*/2)]^* \underset{\tau}{\otimes} [n^*(\tau)\, h''(\tau) \sqcap\!\sqcup (\tau;T^*/2)]\}/T_F^2 \ ,$$

$$B(\tau) = E\{[h'^*(-\tau) n'(-\tau) \sqcap\!\sqcup (-\tau;T^*/2)]^* \underset{\tau}{\otimes} [h'^*(\tau) n'(\tau) \sqcap\!\sqcup (\tau;T^*/2)]\}/T_F^2 \ ,$$

$$B'(\tau) = E\{[h'^*(\tau) n'(\tau) \sqcap\!\sqcup (\tau;T^*/2)]^* \underset{\tau}{\otimes} [h'^*(\tau) n'(\tau) \sqcap\!\sqcup (\tau;T^*/2)]\}/T_F^2 \ ,$$

$$C(\tau) = E\{[n^*(-\tau) n'(-\tau) \sqcap\!\sqcup (-\tau;T_F/2)]^* \underset{\tau}{\otimes} [n^*(\tau) n'(\tau) \sqcap\!\sqcup (\tau;T_F/2)]\}/T_F^2 \ ,$$

$$C(\tau) = E\{[n^*(\tau) n'(\tau) \sqcap\!\sqcup (\tau;T_F/2)]^* \underset{\tau}{\otimes} [n^*(\tau) n'(\tau) \sqcap\!\sqcup (\tau;T_F/2)]\}/T_F^2 \ .$$

(Eq. D.14)

Consider evaluation of $C(\tau)$ and $C'(\tau)$ first, since these are the easiest:

$$C(\tau) = \int_{-\infty}^{\infty} \sqcap\!\sqcup (\tau+\sigma;T_F/2) \sqcap\!\sqcup (\sigma;T_F/2)\, E[n(\tau+\sigma)^* n(\sigma)]\, E[n'^*(-\tau+\sigma) n'(\sigma)]\, d\sigma/T_F^2 \ ,$$

$$= \frac{\sigma_n^4}{T_F^2} \int_{-\infty}^{\infty} \sqcap\!\sqcup (\tau+\sigma;T_F/2) \sqcap\!\sqcup (\sigma;T_F/2)\, \mathrm{sinc}^2(\pi B\tau) e^{-2\pi j \Delta f^o \tau}\, d\sigma \ ;$$

$$\approx \frac{\sigma_n^4}{T_F} \mathrm{sinc}^2(\pi B\tau)\, e^{-2\pi j \Delta f^o \tau} \qquad \text{(Eq. D.15)}$$

and

$$C'(\tau) = \int_{-\infty}^{\infty} \Lambda(\tau-\sigma;\ T_F/2)\Lambda(\sigma;T_F/2)\ E[n(\tau-\sigma)n^*(\sigma)]\ E[n'^*(\tau-\sigma)n'(\sigma)]d\sigma/T_F^2 \ ,$$

$$= \frac{\sigma_n^4}{T_F^2} \int_{-\infty}^{\infty} \Lambda(\tau-\sigma;T_F/2)\Lambda(\sigma;T_F/2)\mathrm{sinc}^2[\pi B(\tau-2\sigma)]e^{-2\pi j\Delta f^o(\tau-2\sigma)}\ d\sigma \ ,$$

$$\approx \frac{\sigma_n^4(B-|\Delta f^o|)}{2B^2\ T_F^2}\ \Lambda(\tau,T_F) \qquad \text{(Eq. D.16)}$$

since $n(\tau)$ and $n'(\tau)$ are independent and BT_F is small compared with unity.

The fourier transforms of C and C' are

$$\mathcal{F}[C(\tau)] \approx \frac{\sigma_n^4}{BT_F}\Lambda(f+\Delta f^o;B)(1-|f+\Delta f^o|/B) \ ,$$

$$\mathcal{F}[C'(\tau)] \approx \frac{\sigma_n^4(B-|\Delta f^o|)}{B^2\ T_F}\ \mathrm{sinc}(2\pi fT_F) \ . \qquad \text{(Eq. D.17)}$$

In the same manner it may be shown that since BT^* is large compared with unity

$$\mathcal{F}[B(\tau)] \approx S/N\ \frac{\sigma_n^4}{BT_F}\ \Lambda[f+(\alpha_o-1)f_o/2+\Delta f_o;|\alpha_o-1|f_o/2\ ,\ B-|\alpha_o-1|f_o/2]$$

$$\mathcal{F}[B'(\tau)] \approx S/N\ \frac{\sigma_n^4}{BT_F}\ \mathrm{sinc}(2\pi fT^*)\Lambda[(\alpha_o-1)f_o/2+\Delta f_o;|\alpha_o-1|f_o/2,B-|\alpha_o-1|f_o/2]$$

$$\mathcal{F}[A(\tau)] \approx S/N\ \frac{\sigma_n^4}{BT_F}\ \Lambda[f-(\alpha_o-1)f_o/2+\Delta f_o;|\alpha_o-1|f_o/2\ ,\ B-|\alpha_o-1|f_o/2]$$

$$\mathcal{F}[A'(\tau)] \approx S/N\ \frac{\sigma_n^4}{BT_F}\ \mathrm{sinc}(2\pi fT^*)\Lambda[-(\alpha_o-1)f_o/2+\Delta f_o;|\alpha_o-1|f_o/2,B-|\alpha_o-1|f_o/2]$$

(Eq. D.18)

where

$$\sqcap(f;\, F_1,\, F_2) = \begin{cases} 1 & |f| \le F_1 \\ 0 & |f| \ge F_2 \\ (F_2-f)/(F_2-F_1) & \text{otherwise} \end{cases} . \qquad \text{(Eq. D.19)}$$

With these results $E[|\delta Y(f)|^2]$ and $E[\delta^* Y(-f)\delta Y(f)]$ are readily determined. For $f = 0.6/T^*$ they may be further approximated to:

$$E[|\delta Y(f)|^2] \approx \frac{(S/N)^2\, \sigma_n^4}{B\, T_F} \left[\frac{B-|\alpha_o-1|f_o-|\Delta f^o/2|}{B-|\alpha_o-1|\, f_o} \; \frac{2}{S/N} + \frac{B-|\Delta f^o|}{B} \frac{1}{(S/N)^2} \right]$$

$$\approx \frac{(S/N)^2\, \sigma_n^4}{B\, T_F} \left[\frac{2}{S/N} + \frac{1}{(S/N)^2} \right] \qquad \text{(Eq. D.20)}$$

Since BT^* is large compared with unity and sinc (1.2π) and sinc $(1.2\pi\, T_f/T^*)$ are negligible. The final result is thus Eq. 20, since $0.43\pi \sqrt{2} \approx 2$. These results differ from those of Plaisant for several reasons: In the first place he assumed $T_F \triangleq \Delta\tau_d$, in the second place he approximated $E\{[|Y(f)|-|Y_e(f)|]^2\}$ by $E[|\delta Y(f)|^2]$ instead of by the correct $E[|\delta Y(f)|^2]/2$.

D.2 Correlation in time

The procedure to be followed is the same, except that the roles of time and frequency are reversed. Obviously this procedure must yield the same approximate variance at half-correlation-peak points since the variation at the correlation peak is used; furthermore, the covariance between the half-correlation-peak points is again approximately zero. However, in the *expected correlation function*, sinc $(\pi f\, T^*)$ must be replaced by sinc $[\pi\tau(B-|\alpha_o-1|f_o-|\Delta f^o|]$, since $B-|\alpha_o-1|f_o$ is the analog of T^* ; therefore, in the slope, T^* must be replaced by $B-|\alpha_o-1|f_o$ and it becomes

$$0.43\, \pi\, S/N\, \sigma_n^2 (B-|\alpha_o-1|f_o-|\Delta f^o|)^2/(B-|\alpha_o-1|f_o) \qquad \text{(Eq. D.21)}$$

The final result is thus Eq. D.21.

D.3 Phase of the Peak

To measure the phase at the maximum magnitude of double correlation it is necessary only to take the arctangent of the ratio of the imaginary part to the real part of the double correlation at this point. The error in measuring phase is just the variation in correlation perpendicular to the expected correlation divided by the magnitude of the expected correlation. But the variance of the correlation in this direction is, following the reasoning of D.1, just one-half the total variance of the correlation $E[|\delta Y(f)|^2]$, which is given at the end of Sect. D.1. If the square root of half this quantity is divided by the magnitude of the expected maximum correlation, which from the beginning of Sect. D.1 is $S/N\ \sigma_n^2\ (B-|\alpha_o-1|f_o-|\Delta f^o|)/(B-|\alpha_o-1|f_o)$, the result is Eq. 44 of the main text.

INITIAL DISTRIBUTION

	Copies
MINISTRIES OF DEFENCE	
MOD Belgium	2
DND Canada	10
CHOD Denmark	8
MOD France	8
MOD Germany	15
MOD Greece	11
MOD Italy	10
MOD Netherlands	12
CHOD Norway	10
MOD Portugal	5
MOD Turkey	5
MOD U.K.	16
SECDEF U.S.	61
NATO AUTHORITIES	
Defence Planning Committee	3
NAMILCOM	2
SACLANT	10
SACLANTREPEUR	1
CINCWESTLANT/COMOCEANLANT	1
COMIBERLANT	1
CINCEASTLANT	1
COMSUBACLANT	1
COMMAIREASTLANT	1
SACEUR	2
CINCNORTH	1
CINCSOUTH	1
COMNAVSOUTH	1
COMSTRIKFORSOUTH	1
COMEDCENT	1
COMMARAIRMED	1
CINCHAN	1

	Copies
SCNR FOR SACLANTCEN	
SCNR Belgium	1
SCNR Canada	1
SCNR Denmark	1
SCNR Germany	1
SCNR Greece	1
SCNR Italy	1
SCNR Netherlands	1
SCNR Norway	1
SCNR Portugal	1
SCNR Turkey	1
SCNR U.K.	1
SCNR U.S.	2
SECGEN Rep. SCNR	1
NAMILCOM Rep. SCNR	1
NATIONAL LIAISON OFFICERS	
NLO Canada	1
NLO Denmark	1
NLO Germany	1
NLO Italy	1
NLO U.K.	1
NLO U.S.	1
NLR TO SACLANT	
NLR Belgium	1
NLR Canada	1
NLR Denmark	1
NLR Germany	1
NLR Greece	1
NLR Italy	1
NLR Netherlands	1
NLR Norway	1
NLR Portugal	1
NLR Turkey	1
NLR UK	1
NLR US	1
Total initial distribution	236
SACLANTCEN Library	10
Stock	34
Total number of copies	280